REPORT DOCUMENTATION PAGE

The public reporting burden for this collection of information is estimated to average 1 hour per response, including the time for reviewing instructions, searching existing data sources, gathering and maintaining the data needed, and completing and reviewing the collection of information. Send comments regarding this burden estimate or any other aspect of this collection of information, including suggestions for reducing the burden, to Department of Defense, Washington Headquarters Services, Directorate for Information Operations and Reports (0704-0188), 1215 Jefferson Davis Highway, Suite 1204, Arlington, VA 22202-4302. Respondents should be aware that notwithstanding any other provision of law, no person shall be subject to any penalty for failing to comply with a collection of information if it does not display a currently valid OMB control number.
PLEASE DO NOT RETURN YOUR FORM TO THE ABOVE ADDRESS.

1. REPORT DATE (DD-MM-YYYY)	2. REPORT TYPE	3. DATES COVERED (From - To)
18/Mar/2002	THESIS	

4. TITLE AND SUBTITLE
DETECTION OF POLYCLIC AROMATIC HYDROCARBON ADDUCTS USING ELECTROCHEMISTRY/ELECTROSPRAY-MASS SPECTORMETRY

5a. CONTRACT NUMBER

5b. GRANT NUMBER

5c. PROGRAM ELEMENT NUMBER

6. AUTHOR(S)
CAPT PFAHLER DAVID A

5d. PROJECT NUMBER

5e. TASK NUMBER

5f. WORK UNIT NUMBER

7. PERFORMING ORGANIZATION NAME(S) AND ADDRESS(ES)
UNIVERSITY OF FLORIDA

8. PERFORMING ORGANIZATION REPORT NUMBER
CI02-38

9. SPONSORING/MONITORING AGENCY NAME(S) AND ADDRESS(ES)
THE DEPARTMENT OF THE AIR FORCE
AFIT/CIA, BLDG 125
2950 P STREET
WPAFB OH 45433

10. SPONSOR/MONITOR'S ACRONYM(S)

11. SPONSOR/MONITOR'S REPORT NUMBER(S)

12. DISTRIBUTION/AVAILABILITY STATEMENT
Unlimited distribution
In Accordance With AFI 35-205/AFIT Sup 1

13. SUPPLEMENTARY NOTES

14. ABSTRACT

20020523 152

15. SUBJECT TERMS

16. SECURITY CLASSIFICATION OF:			17. LIMITATION OF ABSTRACT	18. NUMBER OF PAGES	19a. NAME OF RESPONSIBLE PERSON
a. REPORT	b. ABSTRACT	c. THIS PAGE		87	19b. TELEPHONE NUMBER (Include area code)

DETECTION OF POLYCLIC AROMATIC HYDROCARBON ADDUCTS USING
ELECTROCHEMISTRY/ELECTROSPRAY–MASS SPECTROMETRY

By

DAVID AARON PFAHLER

A THESIS PRESENTED TO THE GRADUATE SCHOOL
OF THE UNIVERSITY OF FLORIDA IN PARTIAL FULFILLMENT
OF THE REQUIREMENTS FOR THE DEGREE OF
MASTER OF SCIENCE

UNIVERSITY OF FLORIDA

2002

TABLE OF CONTENTS

Abstract of Thesis Presented to the Graduate School
of the University of Florida in Partial Fulfillment of the
Requirements for the Degree of Master of Science

DETECTION OF POLYCYCLIC AROMATIC HYDROCARBON ADDUCTS USING
ELECTROCHEMISTRY/ELECTROSPRAY-MASS SPECTROMETRY

By

David Aaron Pfahler

May 2002

Chair: John R. Eyler
Cochair: Anna Brajter-Toth
Department: Chemistry

Electrochemistry (EC) and Electrospray Ionization (ESI) mass spectrometry were coupled online to detect the formation of adducts between polycyclic aromatic hydrocarbons (PAHs) and biological nucleophiles. A simple tubular electrode electrochemical cell was used to oxidize anthracene and benzo[a]pyrene, and a mass spectrometer was used to detect their reaction products. An optimum electrolyte concentration was determined for detecting adducts of anthracene. A lower limit of detection for anthracene adducts was demonstrated for the EC/ESI technique over ESI alone. Several operating parameters were also investigated for optimal PAH adduct detection: the flow rate of the solution, the high voltage applied to the ESI needle, the voltage applied to the capillary, and the collection time in the hexapole.

The nucleophilic reactions of both anthacene and benzo[a]pyrene were investigated using pyridine as a model biological nucleophile. Pyridine adducts were detected for both PAHs. Both adducts demonstrated the loss of one hydrogen from the PAH to give mass-to-charge ratios of one atomic mass unit less than the combination of their molecular weights.

The nucleophilic reaction of anthracene with the base guanine was attempted. The solubility of guanine was a major hurdle, and guanine concentrations used were likely too low. Mass spectrometric peaks observed at the mass of the suspected adduct were below the level of the noise and could not be verified.

The nucleophilic reaction of benzo[a]pyrene with the nucleoside guanosine was also studied. Due to greater solubility, higher guanosine concentrations were used than could be used with guanine. When the electrochemical cell was operated at 5.0 V a small peak was observed at m/z 534. It is suggested that this peak is due to the adduct of a benzo[a]pyrene radical cation with the C8 carbon of a protonated guanosine.

CHAPTER 1
INTRODUCTION

The purpose of this research was to explore the possibility of generating adducts of polycyclic aromatic hydrocarbons (PAHs) and deoxyribose nucleic acid (DNA) bases and detecting them online with the emerging technique known as Electrochemistry/Electrospray Ionization Mass Spectrometry (EC/ESI-MS). This thesis begins with an introduction to PAH molecules and the role of their DNA adducts in carcinogenesis. Chapter 2 explains the development and the applications of Electrochemistry/Mass Spectrometry (EC-MS) and its enhancement through the development of the Electrospray Ionization (ESI) liquid interface technique. Chapter 3 contains information on the instruments and methods used to conduct this research, and Chapter 4 presents the results of the research and discusses their interpretation.

PAH Molecules

Polycyclic aromatic hydrocarbons are a broad class of organic compounds whose structures are based on fused carbon rings. The carbon rings are aromatic, meaning that the π bonding electrons are delocalized over the entire ring, which makes the rings energetically stable. Each carbon atom in the ring structures is sp^2 hybridized. Carbons that are not shared between two rings have one hydrogen atom bound to them. The structures and molecular weights (MW) of the two PAHs, anthracene and benzo[a]pyrene (B[a]P), used in this study are shown in Figure 1.1.

PAH molecules are formed during the incomplete combustion of organic compounds, particularly of fossil fuels [Solomons, 1992]. Because of the stability of their

1
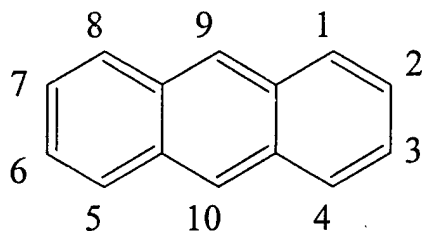
(a)　Anthracene

MW　178
$E_{ap}{}^a$　1.231
IP^b　7.43
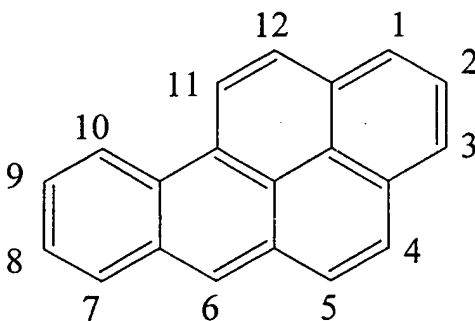
(b)　Benzo[a]pyrene

MW　252
$E_{ap}{}^a$　1.121
IP^b　7.23

Figure 1.1. Structure of PAHs used in study (a) Anthracene (b) Benzo[a]pyrene
[a]Anodic peak potentials (E_{ap}) are expressed in V vs Ag/AgCl and were determined by cyclic voltammetry in dimethylformamide. [b]Ionization potentials (IP) are expressed in eV and were obtained from charge-transfer complex formation with chloranil [Cremonesi *et al.*, 1992].

ring structure, PAH molecules, especially those containing five or more rings, tend to be difficult to degrade in the natural environment [Sawyer *et al.*, 1994]. Many individual PAHs have been shown to have carcinogenic properties in experimental animals and humans, and have been listed among the Environmental Protection Agency's Priority Pollutants [Sawyer *et al.*, 1994]. Reports of cancer development in those who worked with tar and coal products began to surface in the late 1800s [Searle ed.,1976]. The first carcinogenic PAH to be identified was B[a]P which was isolated from coal tar in the 1930's [Cook, 1933]. Since then, a vast body of research has been generated studying PAHs and their cancer causing properties.

PAH-DNA Adducts

In 1964, Brookes and Lawley demonstrated the relationship between the carcinogenic potential of six PAH molecules and the extent to which they became bound in mouse skin DNA [Brookes and Lawley, 1964]. Further research led to the fundamental concept that the covalent binding of PAH to cellular macromolecules such as DNA is the first step in the process leading to tumor initiation [Miller, 1970]. The formation of PAH-DNA adducts had been implicated in cancer initiation, and research was begun to understand the process. An early experiment showed that when B[a]P and various B[a]P metabolites were exposed to liver microsomes and DNA, one particular metabolite became bound to DNA 10 times more than B[a]P itself [Borgen *et al.*, 1973]. PAH molecules have a noticeable lack of reactive sites, and it soon became clear that most PAH carcinogens require metabolic activation before they begin to interact with cellular macromolecules [Miller and Miller, 1981]. Most carcinogenic chemicals require metabolic activation to electrophilic intermediates that react with cellular nucleophiles. For PAH molecules, this metabolic activation can occur by two pathways. The first path is the mono-oxygenation

of the PAHs to produce bay-region diol epoxides [Conney, 1982]. The second path, and the one that this research examined, is the one-electron oxidation of PAHs to give reactive intermediate radical cations [Cavalieri and Rogan, 1984].

Rogan *et al.* structurally characterized the PAH adducts that were electrochemically synthesized when B[a]P underwent a one-electron oxidation in the presence of guanosine [Rogan *et al.*, 1988]. The reaction was carried out by exhaustive electrolysis of B[a]P dissolved in dimethylformamide (DMF) in an electrochemical cell with guanosine in a 10-fold excess. Adducts generated in this reaction were separated and then structurally identified using ultraviolet spectroscopy, nuclear magnetic resonance and mass spectrometry techniques. Adducts of B[a]P were found at the C8 and N7 positions of guanosine and also of guanine following the loss of the sugar moiety from guanosine. The guanosine adduct structures that were identified are shown in Figure 1.2.

The synthesis of PAH-DNA base adducts by one-electron oxidation of PAHs has also been demonstrated using enzymatic oxidants such as horseradish peroxidase [Rogan *et al.*, 1988], prostaglandin H synthase [Devanesan *et al.*, 1987], and cytochrome P-450 [Cavalieri *et al.*, 1990] as well as the chemical oxidant iodine [Hanson *et al.*, 1998]. If this one-electron oxidation is indeed a pathway for adduct formation, then one factor in predicting the carcinogenic potential of a PAH should be how easily an electron is removed from the PAH. The correlation of the ionization potentials (IP) of PAHs with the extent of their binding to DNA was first demonstrated in 1983 [Cavalieri *et al.*, 1983]. This correlation was later extended to the anodic peak potentials (E_{ap}) of PAHs [Cremonesi *et al.*, 1992].
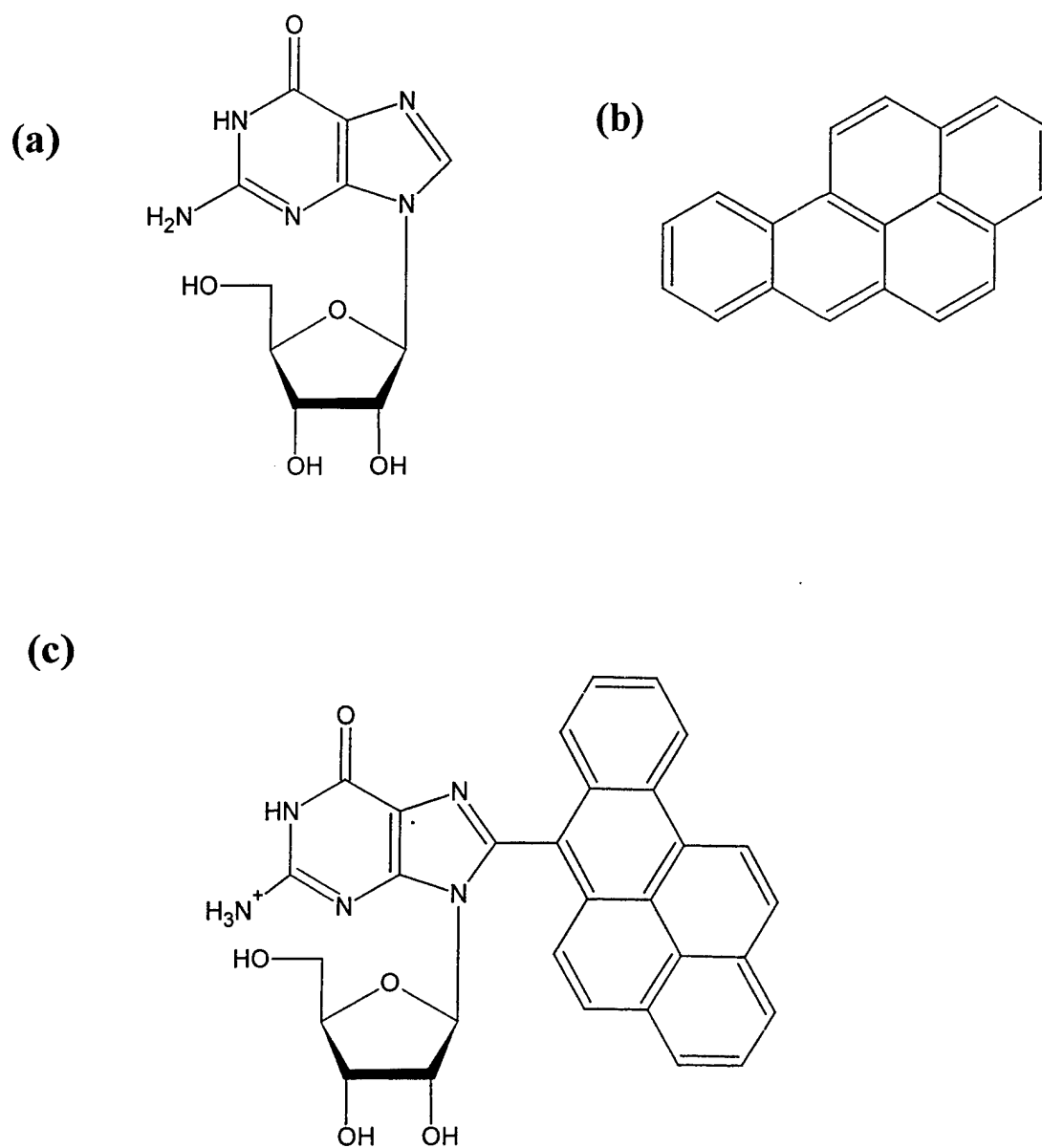
Figure 1.2. Structure of B[a]P-guanosine adduct. (a) Guanosine, MW 283
(b) Benzo[a]pyrene, MW 252 (c) Guanosine-B[a]P adduct. The major identified
adduct of the electrochemical reaction was detected as [M+H]$^+$ at m/z 534 [Rogan *et
al.*, 1988].

demonstrating that a low IP and E_{ap} are necessary characteristics for binding of PAHs to occur by the one-electron oxidation pathway.

DNA Adducts in Cancer Research

The danger in the formation of DNA adducts in living cells is that adducts can hinder the proper functioning of the DNA. Adducted bases can cause the misincorporation or slippage by DNA polymerase as it replicates a DNA strand, or the adducted base can be replaced with the wrong base in a DNA repair process [Hemminki *et al.*, 2000]. Both of these events cause a mutation in the DNA strand. The presence of DNA adducts in a biological tissue may increase mutations, but this does not necessarily imply that there is an increase in cancer risk for that tissue [Nestmann *et al.*, 1996]. Evidence of this is suggested by the fact that DNA adducts are often found in both target and non-target tissues [Walker *et al.*, 1992]. Instead, it appears that adducts are linked to cancer only when they cause mutations in genes that regulate cell growth and act as tumor suppressors [Fearon, 1997]. However, measuring the existing levels of DNA adducts in tissues does show promise as a way of gauging exposure to carcinogens and may be useful in predicting human cancer risks [Hemminki *et al.*, 2000].

Analytical Techniques for DNA Adduct Studies

Our knowledge of how DNA adducts affect living organisms relies on the detection, quantification, and characterization of these adducts. Testing for DNA adduct formation first requires that either DNA, cultured cells, experimental animals, or even human tissues be exposed to carcinogens. Highly sensitive methods are then required to detect

the occurrence of DNA adducts. Several different techniques have been successfully used for adduct detection and quantification and are discussed below.

Treating a sample with radioactively labeled carcinogens is the oldest method of adduct detection [Kriek *et al.*, 1998]. DNA from the treated sample is extracted, purified, and measured for its radioactivity by either liquid scintillation counting or accelerator mass spectrometry [Reddy, 2000]. Detection of radioactivity denotes the formation of adducts for that compound. Radiolabeling is straightforward, but it is expensive and cannot be performed with human subjects. There are also complications with assuring the radioactive label has not been lost or incorporated into unmodified DNA [Reddy, 2000].

In ^{32}P-postlabeling, the radioactive tag is applied after DNA adduct formation. After treatment with a carcinogen, adducted DNA is digested to its mononucleotides. The adducted nucleotides are enriched, and then they are enzymatically labeled with ^{32}P. Labeled nucleotides are separated by thin layer chromatography and detected by exposure of X-ray films or electronic autoradiography [Reddy, 2000]. This technique is very sensitive, detecting 1 adduct in 10^9 unmodified nucleobases and requiring only 2-10 µg of DNA [Kriek *et al.*, 1998]. Its main drawback is that it is a time and labor-intensive technique. In addition, it cannot differentiate between or provide any structural information for detected adducts.

Immunoassy [Lunn *et al.*, 1997], fluorescence spectroscopy [Rojas *et al.*, 1994], and mass spectrometry [Chaudhary *et al.*, 1994] have all been applied successfully to adduct detection and quantitation as well. Of these five methods, only mass spectrometry has the ability to provide structural information for adducts, done through tandem MS [Iannitti-Tito *et al.*, 2000]. MS can also offer sensitivity approaching that of the ^{32}P-

postlabeling technique [Roberts *et al.*, 2001]. Recently, a liquid chromatography electrospray tandem mass spectrometry (LC-ESI-MS/MS) technique has been developed with sufficient sensitivity that it can be used for monitoring the low level of adducts formed in chronically dosed animals [Walton *et al.*, 2001].

Testing Compounds for DNA Adduct Formation

Over 800 chemicals have been tested for their overall carcinogenicity. Of these, 75 have been demonstrated to be human carcinogens and 15 of those have been shown to bind to DNA *in vitro* [Hemminki *et al.*, 2000]. The analytical methods outlined above can be used to screen untested compounds to determine whether they, or one of their metabolites, have the potential to react with DNA. These methods are all based on the dosing of a DNA test sample with the compound and then looking for resulting adducts using a specific analytical method.

In the research reported in this thesis, I looked at the possibility of using a new technique for screening PAH compounds for adduct formation. PAHs are electrochemically oxidized in solution with DNA bases or nucleosides. The oxidation step takes the place of the metabolic activation of PAHs in living cells. The oxidized compound can undergo nucleophilic reactions with the DNA base in solution. Resulting reaction products are ionized using a soft electrospray ionization technique and then detected using mass spectrometry. This method might be used as a preliminary approach to determining the genotoxicity of an untested compound. A sample run could be accomplished in minutes and could give a preliminary indication of compounds that may form DNA adducts *in vivo* without having to dose a DNA sample. If this technique is

successfully applied to PAH adducts, it may be further extended to screen other compounds that metabolize via oxidation steps in the body.

CHAPTER 2
ELECTROCHEMISTRY/ELECTROSPRAY-MASS SPECTROMETRY

Introduction

Electrochemistry combined with mass spectrometry (EC/MS) builds on the strengths of two analytical methods to offer new insight into oxidation and reduction (redox) reactions. Electrochemical cells are used to initiate and control redox reactions [Bard and Faulkner, 1980]. When coupled with a mass spectrometer, the resulting mixture of reactants, intermediates, and products can be mass analyzed relatively quickly to identify and monitor concentrations of individual species throughout the reaction [Volk *et al.*, 1992]. The mass spectrometer is an ideal detector for electrochemistry since all compounds, upon ionization, produce a signal [Niessen, 1999]. In EC/MS, a flow-through electrochemical cell is interfaced with the mass spectrometer to produce an online technique. Coupling online provides the time resolution needed to detect the transient intermediates of fast redox reactions [Volk *et al.*, 1992]. Furthermore, intermediates or products can be monitored selectively by using MS/MS methods. This gives EC/MS the versatility of analyzing complex reactions without having to first separate analytes, intermediates, and products [Volk *et al.*, 1992].

In the past ten years, Electrospray Ionization (ESI) has developed into the method of choice for transferring compounds in solution into the gas phase environment of the mass spectrometer [Cole, ed., 1997]. Recently, the electrolytic nature of the ESI interface itself has been explored as a way to ionize compounds electrochemically [Van Berkel *et al.*, 1992]. An EC cell can be combined with ESI to increase ionization efficiency in a

10

technique known as Electrochemistry/Electrospray Ionization Mass Spectrometery (EC/ESI-MS) [Zhou and Van Berkel, 1995]. EC/ESI-MS was used in this study to generate radical cations of polycyclic aromatic hydrocarbons, and to detect these radical cations and their reaction products. This chapter traces the development of EC/ESI-MS from its roots in ES/MS and ESI, and then considers some instrumental considerations for the ionization of PAHs. The chapter concludes by covering selected applications of EC/ESI-MS that highlight its potential for use in screening untested compounds for low levels of DNA adducts.

<p align="center">**Development of EC/ESI-MS**</p>

Development of EC-MS

The greatest difficulty to overcome in coupling electrochemistry to mass spectrometry is interfacing the liquid phase of electrochemical cells with the high vacuum environment of the mass spectrometer. Bruckenstein and Gadde accomplished the first combination of an electrochemical cell online with a mass spectrometer in 1971 [Bruckenstein and Gadde, 1971]. A porous Teflon membrane interface allowed for the monitoring of gaseous products of a reduction reaction at the electrode of the cell. Only volatile intermediates and products of the reactions could be analyzed using membrane interfaces, so the technique was severely limited in its use.

In 1986, Hamitzer and Heitbaum coupled an electrochemical cell to MS detection using the thermospray (TS) liquid interface [Hamitzer and Heitbaum, 1986]. They studied the oxidation of N,N dimethylaniline at a platinum electrode, and were able to observe dimer and trimer products within 10 seconds of generation in the cell. By reducing the dead volume between the cell and the mass spectrometer, Volk et al. were able to cut the delay time in this interface to only 520 milliseconds [Volk et al.,1992].

This short delay time leads to an increased ability to detect short-lived intermediates in mechanistic studies. Volk used this interface to elucidate the oxidation pathway of uric acid [Volk *et al.*, 1992]. The advantage of the TS interface is that it allows for the study of nonvolatile compounds. However, the heat required to vaporize the effluent can alter the kinetics of the reaction and cause thermal decomposition of the analyte or intermediates.

Bartmess and Phillips introduced an electrochemically assisted Fast Atom Bombardment (FAB) interface [Bartmess and Phillips, 1987]. A potential is applied to the FAB probe tip to help in the ionization of previously un-ionizable compounds. Electron transfer reactions were demonstrated directly inside the ionizing source, eliminating any transport delay. However, the high potentials that were required made ion selectivity very difficult, because everything in solution reacted.

Another interface technique which was successfully applied to EC/MS was Particle Beam (PB) ionization, accomplished by Zhang and Brajter-Toth [Zhang and Brajter-Toth, 2000]. In this work the authors detected the radical cation of triphenylamine as well as the dimer tetraphenylbenzidine which was generated in a thin-layer flow-through electrochemical cell.

In 1995, Zhou and Van Berkel demonstrated the coupling of an electrochemical cell with MS via an electrospray interface [Zhou and Van Berkel, 1995]. The ESI interface has several advantages over the techniques discussed above. There is no heating of the solution, therefore thermal decomposition ceases to be an issue. Gas phase reactions of the analyte ions are minimal since the ions are imparted very little energy. Finally, a wider variety of common electrochemistry solvents can be used in the ESI interface

making it a more versatile technique. The following section explores the development of this interface.

Development of Electrospray Ionization

Transfer of ions from solution to the gas phase has been problematic in mass spectrometry. Ions in solution are surrounded by a shell of solvent molecules with which they interact through electrostatic attractions. Overcoming these multiple interactions requires energy to be added to the system. In addition, removing the ion from the solvent shell decreases the order in the solution, resulting in an increase in the entropy of the system. Both of these thermodynamic considerations result in the overall energy required to desolvate an ion being larger than the energy required to break covalent bonds. If this energy is supplied all at once, fragmentation of the analyte will occur. While other liquid to gas-phase ionization methods rely on concentrated energy inputs, ESI relies on low level thermal energy absorbed over time to supply the necessary energy. As a result, fragmentation of the analyte is very low, and a strong molecular ion signal can be generated.

The electrospray interface is based on the dispersion of a liquid into charged droplets by applying a high electrostatic field at the tip of a small nozzle. The droplets shrink through solvent evaporation and droplet fission until individual ions in the droplets are liberated. The first experimental studies of this concept were carried out by Zeleny [1917]. In the late 1960s, Dole proposed to use such an electrostatic sprayer to produce a beam of gas-phase ions from macromolecular ions in solution [Dole *et al.*, 1968]. Dole's group measured the ion current and found it consistent with singly charged ions being liberated from solution. A decade later, the mass spectrometric detection of ions liberated from charged droplets was first reported [Thompson and Iribane, 1979]. However, the

charged droplet source that they used operated on different principles than the electrospray nozzle. It was not until 1984 that two groups, those of Fenn and Alexandrov, independently demonstrated the successful application of an electrospray nozzle as an ion source for mass spectrometry [Yamashita and Fenn, 1984; Alexandrov *et al.*, 1985]. The potential of electrospray ionization (ESI) as an interface for liquid separation techniques was immediately recognized and its use in coupling liquid chromatography (LC) to MS was demonstrated [Whitehouse *et al.*, 1985]. Based on this success, the Smith group began to demonstrate the online coupling of ESI to capillary electrophoresis separations [Olivares *et al.*, 1987; Smith *et al.*, 1988] while the Henion group [Bruins *et al.*, 1987; Covey *et al.*, 1988] continued work on the LC-ESI interface. Both groups demonstrated the successful detection of many types of nonvolatile, polar, and thermally labile compounds which either existed as ions in solution or were ionized using acid-base reactions.

As work to characterize this interface continued, reports began to surface that the products of oxidation reactions were being seen in the mass spectra. The first report was of metal ions that were being oxidized from the capillary itself [Blades *et al.*, 1991]. Molecular radical cation (due to the loss of one electron) of divalent metal porphyrins in solution were subsequently reported [Van Berkel *et al.*, 1991]. It soon became apparent that electrochemical oxidation was occurring as a result of the ESI process. The ESI needle was acting as an electrochemical cell, allowing neutral, nonpolar molecules like PAHs to be ionized and detected as radical cations [Van Berkel *et al.*, 1992].

As the electrochemical nature of the ESI process was being realized, several research groups began coupling electrochemical cells to MS with ESI interfaces and the

EC/ESI-MS technique was born [Bond *et al.*, 1995 ; Zhou and Van Berkel, 1995 ; Xu *et al.*, 1996].

Instrumental Considerations

There are two major areas of concern to be addressed in the coupling of EC to MS via ESI. The first area is the operational configuration of the electrochemical cell and the second is choosing appropriate solvent systems and electrolytes.

Cell Configuations

Connecting the EC cell to the high voltages of ESI can be problematic. The cell circuitry must either be decoupled from this voltage, which leads to long transfer lines and poor response time, or be floated at the high voltage of the ESI needle, which is dangerous for electronic instrumentation [Zhou and Van Berkel, 1995]. The corresponding circuits for these options are shown in Figure 2.1a and 2.1b respectively. Cell circuitry may be set up to operate as either a 2 or 3 electrode systems in either constant current (CCE) or constant potential (CPE) modes. Circuitry schemes for the source are shown in Figure 2.1c and 2.1d respectively. Zhou and Van Berkel also evaluated several electrode geometries for flow-through cells. They tried out thin-layer, tubular, and porous electrode geometries shown in Figures 2.2a, 2.2b, and 2.2c respectively. They found advantages to operating in the 2 electrode CCE mode, citing easier circuitry design, lower necessary electrolyte concentration, and steadier signal response as benefits. Xu *et al.* evaluated a unique 3 electrode cell in which the working electrode is coaxial with the solution flow, but shielded from it up until right before the Taylor cone region of the ESI needle [Xu *et al.*, 1996]. This cell allowed electrolysis of analytes to be performed immediately before they were sprayed, and showed increased sensitivity for the detection of PAH cation radicals when the EC cell was on. Many EC

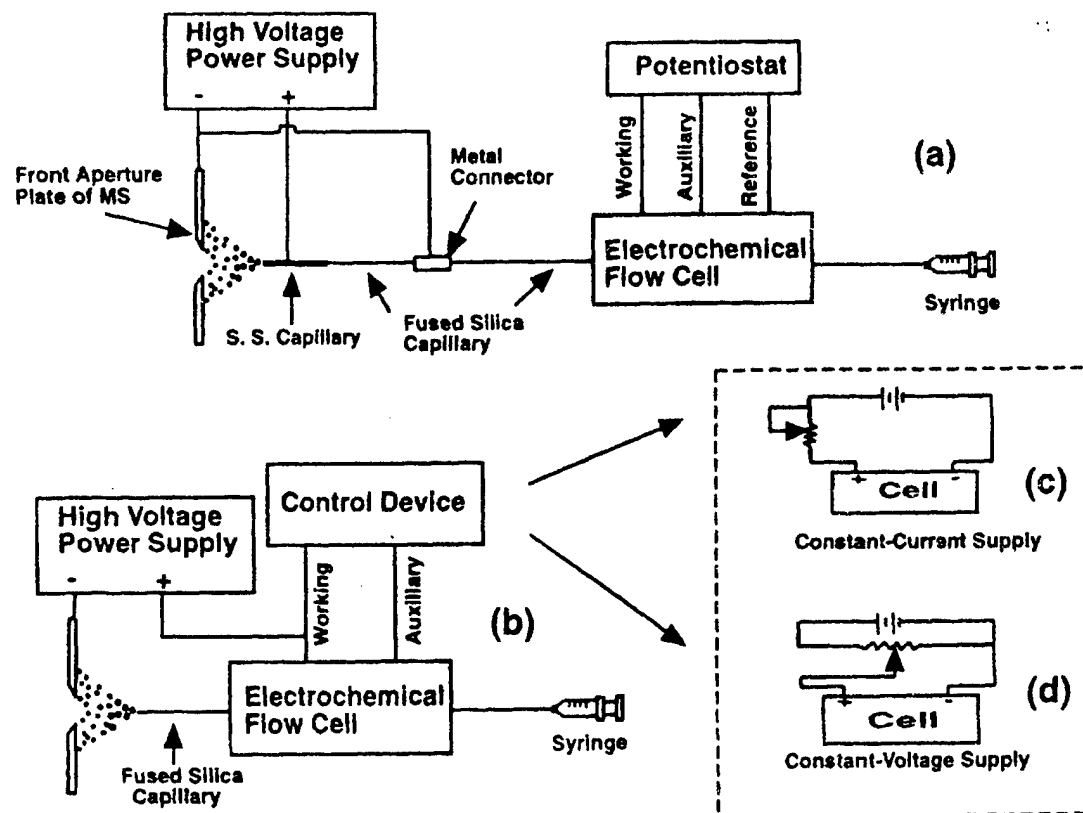**Figure 2.1.** Circuits for EC/ESI-MS. (a) EC cell decoupled from the high voltage of the ESI needle (b) EC cell floated at the high voltage of the ESI needle (c) Constant current supply source (d) Constant voltage supply source [Zhou and Van Berkel, 1995].
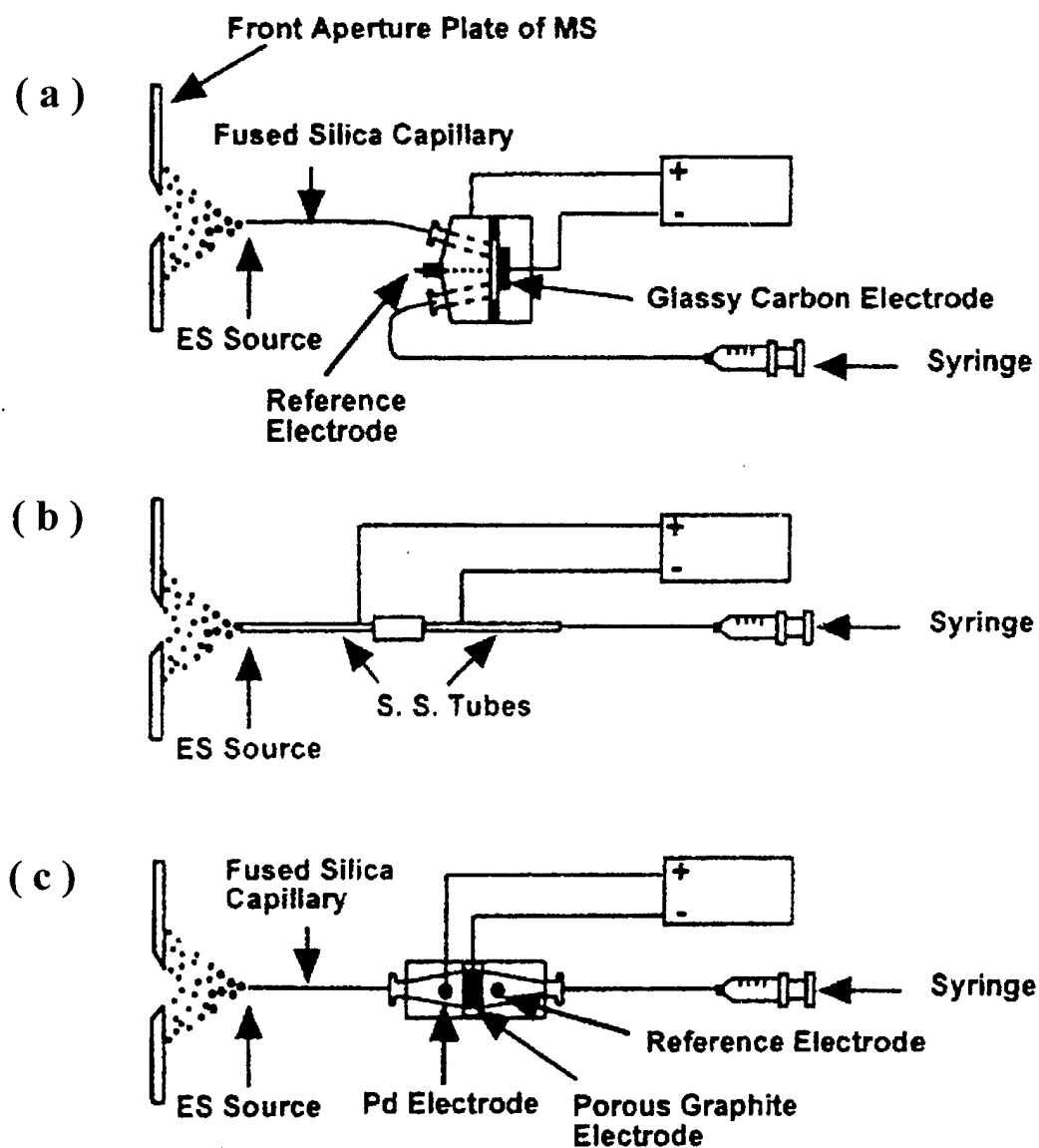
Figure 2.2. Electrode geometry for EC/ESI-MS. (a) thin layer electrode design (b) tubular electrode design (c) porous electrode design [Zhou and Van Berkel, 1995].

cell configurations are possible, the choice will depend ultimately on the application of the device.

Electrolyte Concentration

ESI operates as an essentially current-limited electrolysis cell [Cole ed., 1997]. In standard electrolysis reactions, a 10 to 100-fold excess of electrolyte is added to increase the conductivity of solution [Bard and Faulkner, 1980]. In ESI, the addition of an electrolyte to solution increases the spray current, i_{ES}, which increases the Faradaic current at the needle/solution interface. Electrolyte is also needed in ESI to set up the double layer in solution that allows the formation of the Taylor cone. The electrolyte then is especially important when working with neutral molecules like PAHs. However, electrolyte ions can also interfere with the intended analyte once it is ionized by competing for sites at the surface of the ESI droplets. If the electrolyte ion concentration is too high, and the electrolyte has a greater surface activity than the intended analyte ions, then the analyte signal can be greatly suppressed. The use of high concentrations of nonvolatile electrolytes can also cause problems with plugging and fouling of electrode surfaces. These issues can be resolved by using lower concentration of electrolytes and by choosing electrolytes that have very limited suppression effects. Van Berkel reported success with the use of lithium trifluoromethanesulfonate (LiT) as an electrolyte. The small lithium ion exhibits far less suppression of analyte than common EC electrolytes such as quaternary ammonium salts [Zhou and Van Berkel, 1995].

Solvent

The solvent choice for the ESI solution depends on the analyte in question. Typical analytes for ESI were compounds that exist as ions in solution or that could be ionized in solution by acid/base reactions. They required polar solvents. In contrast, PAHs are

neutral, nonpolar compounds and require nonpolar or low polarity solvents. Hoever, the electrolytes that are needed to achieve sufficient solution conductivity still require polar solvents. Xu *et al.* solved this problem by using a miscible mixture of a polar (acetonitrile) and a nonpolar (methylene chloride) solvent [Xu *et al.*, 1996].

Solvent choice is also driven by the physical characteristics of the solvent. The Cole group, taking into account both the operational requirements of the EC cell and the ESI cell, considered several characteristics [Xu *et al.*, 1996]. Both electrochemical cells require that the solvent be stable within the potential range of the electrochemistry that is occurring. Low viscosity of the solvents is necessary to form a stable spray, and low boiling points are desired to increase the evaporation rate of the solvent from the ESI drops. Solvents with high dielectric constants improve the conductivity of solution. These characteristics ensure a stable ESI signal and good conditions for electrolysis in the ESI needle. Finally, solvents should have low nucleophilicity so that they stabilize the radical cations once they are formed. This is very important when considering the detection of biological adducts, since a nucleophilic solvent will compete with the biological nucleophile. Since the solvent is at such high concentrations, solvent adducts will form preferentially. Table 2.1 compiled by Xu *et al.* summarizes the properties of common electrochemistry solvents.

EC/ESI-MS Applications

EC/ESI-MS has been used in several applications that make it a good choice for generating and detecting PAH-DNA adducts. These selected applications are divided into two categories. The first category deals with the enhancement of analyte signals. The second category is the use of EC/ESI-MS for the detection and the monitoring of redox reactions and their products.

Table 2.1. Properties of Solvents Commonly Used in Electrochemistry

solvent	boiling point (°C)	dielectric const[a]	viscosity at 15 °C (cp)	potential limits (V vs SCE)	nucleophilicity
acetonitrile	81.6	37.5 (25)	0.375	−3.5 to +2.4	moderate
N,N-dimethylformamide	153	36.7 (25)	0.92 (20 °C)	−3.5 to +1.5	moderate
propylene carbonate	241.7	69 (25)		−2.5 to +1.7	moderate
methylene chloride	39.8	9.08 (20)	0.449	−1.7 to +1.8	low
nitromethane	101	36.7 (20)	0.620 (25 °C)	−1.2 to +2.7	
nitrobenzene	210.9	34.82 (25)	2.24		low
methanol	64.7	32.63 (25)	0.623	−2.2 to +1.5	high
water	100	80.10 (20)	1.139	−2.7 to +1.5	high

[a] Numbers in parentheses, temperature (°C).

Source: Xu et al. [1996].

Electrochemical Enhancement of Mass Spectrometry

Zhou and Van Berkel report that EC/ESI-MS can enhance the generation of ions from neutral molecules [Zhou and Van Berkel, 1995]. Although ESI is an inherent electrolysis process, it is current-limited and often electrospray ionization alone is not sufficient to produce a signal from neutral compounds. The EC cell can produce a constant current up to 2 orders of magnitude higher than the ESI nozzle, and can ionize neutral compounds using redox reactions much more efficiently. The careful control of either the EC cell current (CCE mode) or the working electrode potential (CPE mode) should allow for selectivity in the ionization of mixtures of neutral compounds based on their redox potentials. Several authors have described enhanced ionization using EC/ESI-MS for various PAH molecules [Zhou and Van Berkel, 1995; Xu *et al.*, 1996; Palii *et al.*, 2000; Zhang, 2001].

Pretty *et al.* used EC/ESI-MS to apply an electrochemically-modulated pre-concentration and matrix elimination method (EMPM/ES-MS) for the enhancement of the analysis of organic compounds. In this experiment, the choice of electrode material, the system's solvent, and the electrode potential control the non-electrolytic adsorption of the analyte to the electrode. A potential is applied to the EC cell that allows it to adsorb the analyte from solution. The original matrix, which would have interfered with the detection of the analyte, is then washed out of the system while the analyte remains adsorbed. Turning the cell off again releases the analyte back into solution, greatly increasing its concentration and its detection levels. Figure 2.4b demonstrates the cell potentials and signal response for this process. The breast cancer drug tamoxifen and one of its metabolites, 4-hydroxytamoxifen were used for this study and a lowering in detection limit from .2 nM to .025 nM was demonstrated [Pretty *et al.*, 2000].
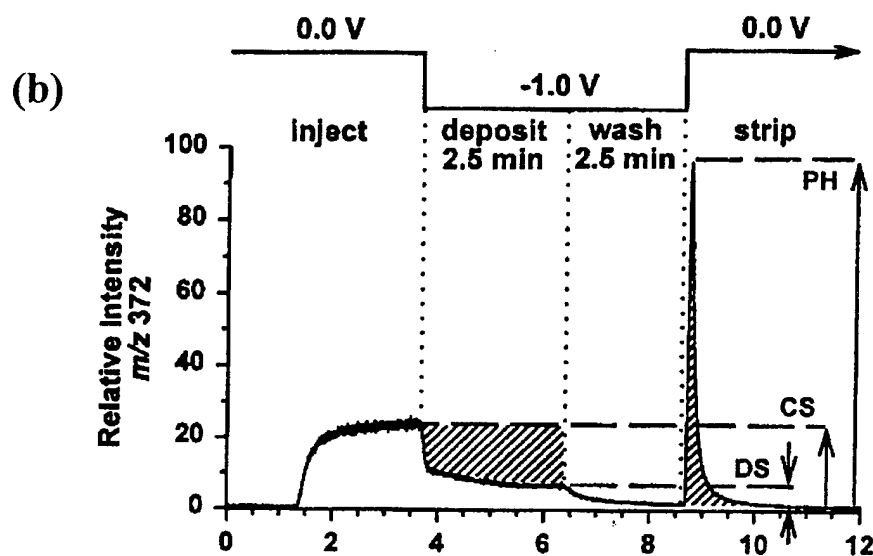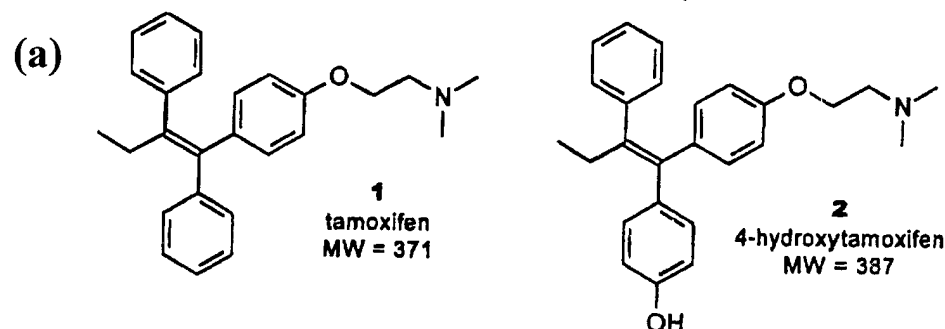
Figure 2.3. EC/ESI-MS used in electrochemically modulated preconcentration and matrix elimination. (a) Analytes used were the breast cancer drug tamoxifen and its major metabolite 4-hydroxytamoxifen (b) A plot of the mass spectrometric response for tamoxifen shows the four steps of the experiment along with corresponding EC voltage changes and solvent wash [Pretty *et al.*, 2000].

Probing Redox Reactions

The combination of EC online with MS serves as an ideal probe of oxidation/reduction reactions. The electrochemical cell generates the conditions necessary to initiate reactions, and the mass spectrometer detects the reactants, intermediates and products. The online aspect of this method allows almost real-time detection, so that even short-lived intermediates can be seen, allowing the elucidation of the reaction pathways of molecules. To identify the individual components, structural information can be obtained using the additional power of MS/MS [Volk *et al.*, 1992]. Zhou and Van Berkel demonstrated the detection of short-lived intermediates of ß-carotene using EC/ESI-MS. Measuring the relative abundance of the mass peaks allowed monitoring of the initial 2-electron oxidation and the rapid follow up reaction [Zhou and Van Berkel, 1995]. Xu *et al.* identified intermediates in the oxidation pathway of the PAH benzo[a]pyrene in a similar study [Xu *et al.*, 1996]. EC/ESI-MS has also been used to study follow up reactions that occur in solution. The nucleophilic addition of pyridine to 9,10-diphenylanthracene was studied and a reaction mechanism was proposed based on the observed mass peaks [Lu *et al.*, 1997].

A recent study [Jurva *et al.*, 2000] evaluates the use of EC/ESI-MS for the study of enzyme catalyzed reactions. This is an area of increasing importance as combinatorial chemistry is used in developing new drugs. Large numbers of new compounds are generated and their metabolism products need to be characterized. Studies done in living tissue (*in vivo*) and done in purified enzyme digests (*in vitro*) can be costly and time consuming. EC/ESI-MS may be a way to simulate drug metabolism quickly and at low cost. In this study the ability of the technique to mimic oxidative (phase I) drug metabolism is investigated. As the voltage of the working electrode is scanned, it reaches

the potential (energy barrier) of a particular reaction, and that oxidation reaction is initiated (in essence catalyzed). In this study the oxidation of the S(-) enantiomer (S-0923) of the dopamine agonist N-0437 [2-(N-propyl-N-2-thienylethylamino)-5-hydroxytetralin] was studied and compared with the known metabolites from an *in vitro* rat liver experiment. The EC/ESI-MS system was able to mimic the first step of oxidative metabolism for the de-alkylation of the tertiary ammine. However, the second step, phenol oxidation, proceeded beyond that which occurs *in vivo*. The resulting oxidation products and their monitoring via mass spectrometry are shown in Figure 2.5a and 2.5b respectively. The results demonstrate that the enzymatic oxidation is more selective than the electrochemical system. However, EC/ESI-MS may still fulfill a vital role in the initial screening of new drugs to predict which metabolites to look for in more precise methods.

Conclusion

As EC/ESI-MS has developed, it has proven to be a useful method for the elucidation of oxidation reaction pathways and determination of subsequent reaction products. PAH molecules are known to be oxidized in the electrochemical cell and their nucleophilic reaction products can be detected using this technique. This technique shows promise, then, for detecting PAH-DNA adducts formed in solution. The techniques outlined in this chapter for the enhancement of analyte signals of both neutral PAHs and organic compounds might be successfully applied to increase the formation or detection of PAH-DNA adducts formed at low levels. If detection of PAH-DNA adducts can be accomplished, the EC/ESI-MS technique might be applied to a wider variety of compounds, especially untested drugs, to elicit their metabolism products and reactivity with biological nucleophiles.
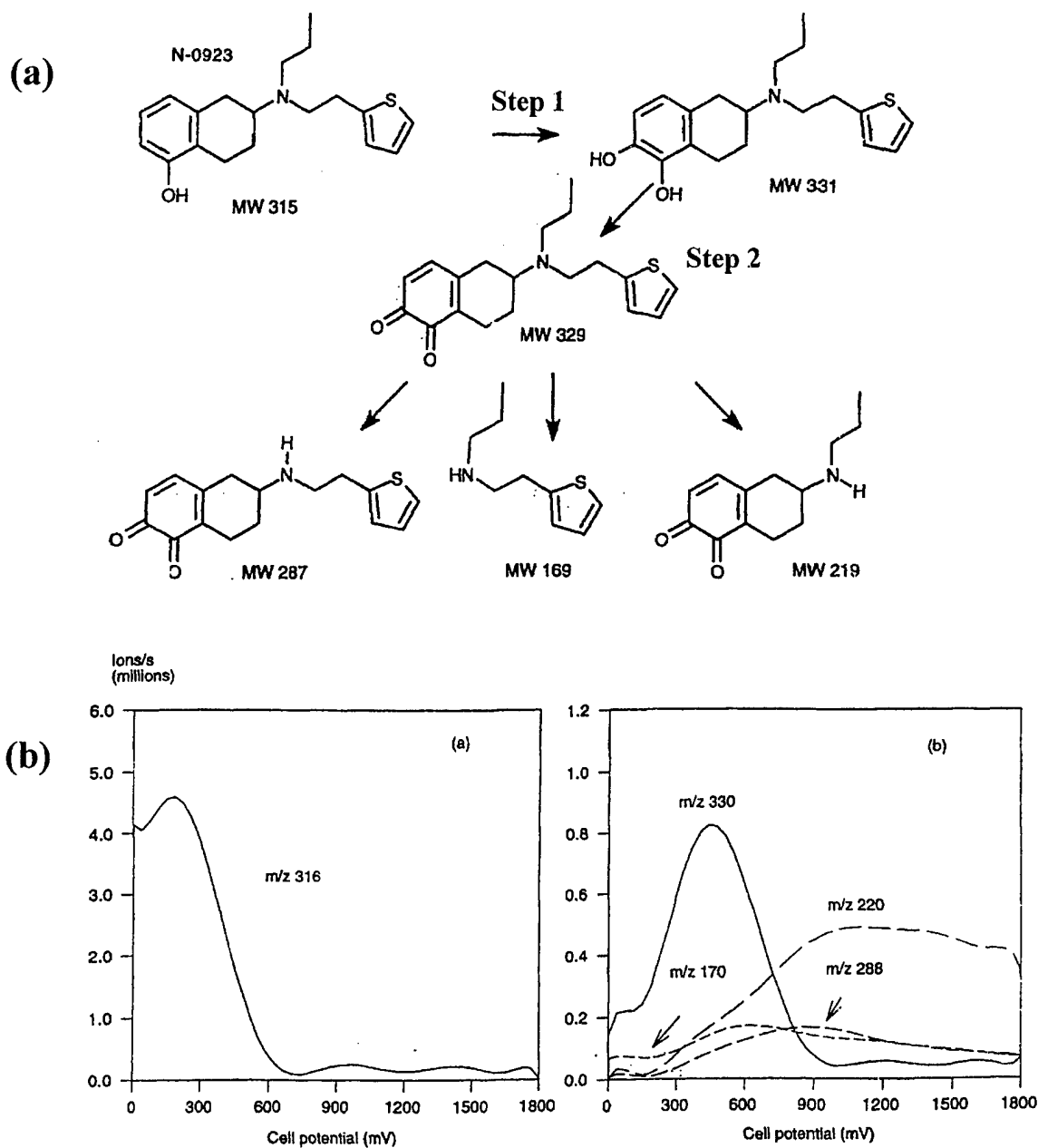
(a)

(b)

Figure 2.4. EC/ESI-MS used in mimicry of phase I drug metabolism. (a) The oxidative pathway for N-0923 observed in the electrochemical cell. Step one corresponds to the metabolites seen in rat liver experiments. Step two procedes beyond the oxidation observed in rat livers. (b) Ion voltammograms showing the production of the psuedo-metabolites of N-0923 [Jurva *et al.*, 2000].

CHAPTER 3
EXPERIMENTAL

Methods and Instrumentation

EC Flow Cell

The EC cell used for this experiment is shown in Figure 3.1. It was designed and built in our group and modeled after the tubular electrode cell designed by Van Berkel's group. [Zhou and Van Berkel, 1995]. It consists of two stainless steel capillary tubes that are joined by a plastic sleeve which holds them 1 mm apart. The inner diameter of the capillaries is 200 μm. The length of the ESI needle section, SS(1), is 52 mm, making the solution volume from the gap where the electrochemical cell is operated to the needle end of the capillary approximately 1.63 μL. At a standard flow rate of 75 μL/h, it will take 1.5 minutes for solution to travel from the EC cell to the ESI tip. The counter electrode for the EC cell is labeled as SS(2).

EC/ESI-MS Parameters

The EC/ESI-MS setup is also shown in Figure 3.1. The EC cell was mounted in front of the inlet capillary of the conventional ESI source using an adjustable three-axis stage. The cell was aligned so that it was perpendicular to the opening of the inlet capillary. The EC cell tip was placed at a distance of 3 mm from the opening in all experiments.

The ESI voltage was brought to the spray needle from the original ESI source (Analytica of Branford, Inc.) using an appropriately rated, insulated copper wire with an
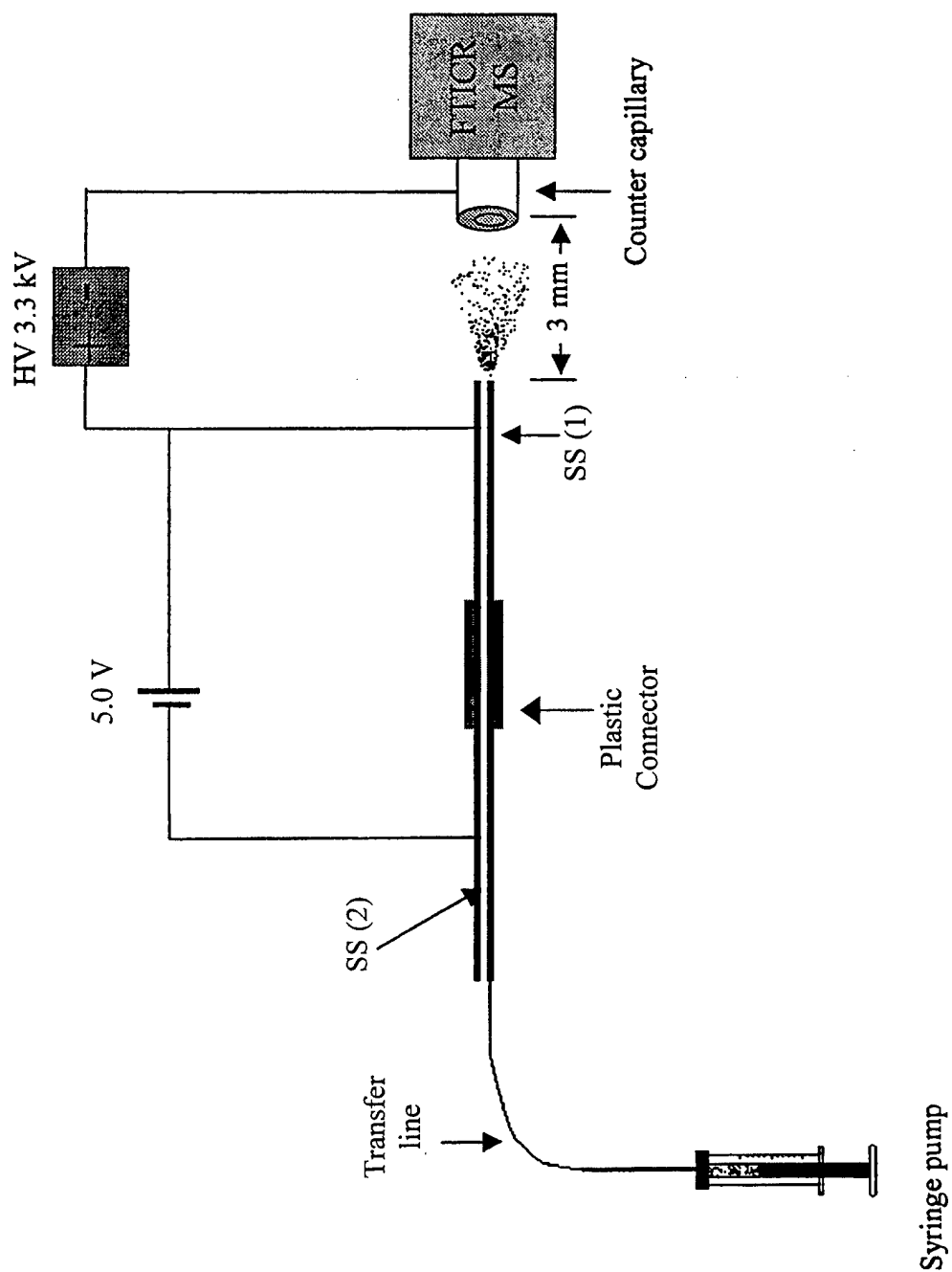
Figure 3.1 Electrochemical cell and instrumental setup for online EC/ESI-MS. SS(1) is the working electrode and the ESI needle. SS (2) is the counter electrode. Adapted from Zhang, [2001].

alligator clip on the end. An ESI variable voltage source (Analytica of Branford, Inc) was used to apply 3300 volts in most experiments unless otherwise specified. The voltage source also housed an amperometer that was used to monitor the ESI current.

The EC cell was connected to a syringe pump (974900 series, Cole Parmer, Vernon Hills, IL) using flexible plastic tubing. Samples were loaded into a Hamilton 250 μL syringe, which was then locked into the syringe pump. Samples were injected continuously, at a flow rate of 75 μL/h unless otherwise specified.

The cell was operated in a constant potential mode. A 9-volt battery supplied the voltage for the EC cell. The battery was floated at the high voltage of the ESI needle. The battery terminals were connected to a voltage divider that was used to control the voltage applied. The voltage divider was attached to the cell via two leads with alligator clips. To switch between the cell on and cell off modes, the alligator clips connecting the battery to the voltage divider were disconnected. For safety reasons, connecting and disconnecting the EC cell was only performed when the ESI voltage had been turned off. Experiments in the EC/ESI mode were conducted at an EC cell voltage of 5.0 V unless otherwise specified.

FTICR-MS

A Bruker APEX 4.7 Tesla FTICR mass spectrometer (Bruker Daltonics, Billerica, MA) was used for high-resolution mass detection. A schematic of the mass spectrometer is shown in Figure 3.2. The FTICR achieved high vacuum using a newly installed turbopumping system. A Pfeiffer 500 L/s and a BOC Edwards 70 L/s turbopump were used to achieve a vacuum of 4.3×10^{-10} mbar in the ICR cell region. The source region
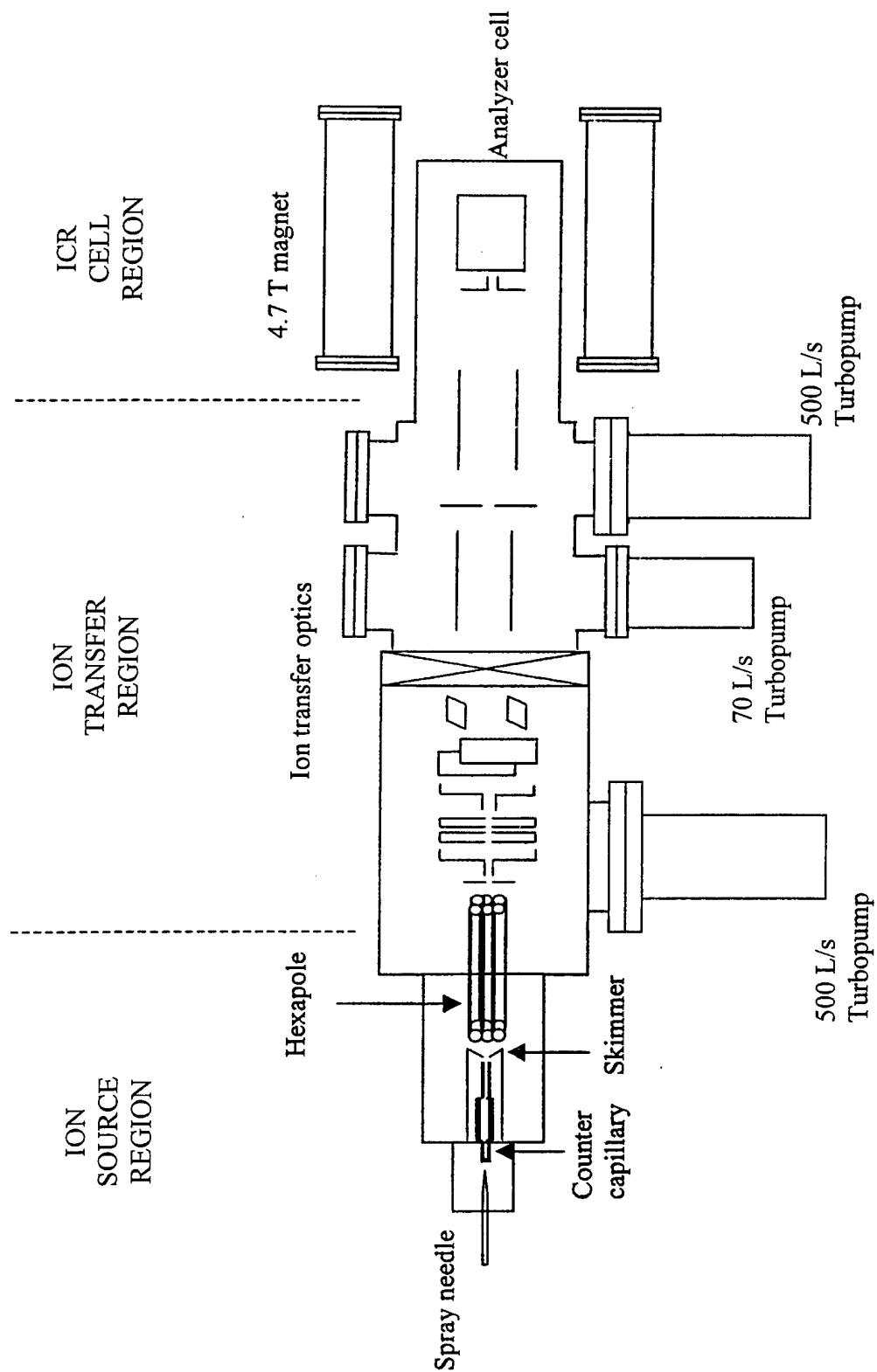
Figure 3.2. Bruker Apex 4.7 FTICR mass spectrometer with external ESI source.

was pumped by a Pfeiffer 500 L/s and a BOC Edwards 250 L/s turbopump and achieved

a vacuum of 5.0 x 10^{-6} mbar under spray conditions.

The voltages applied to the counter capillary and skimmer, the hexapole, ion optics,

and the ICR cell were all controlled from within the Bruker Apex FTICR XMASS

(version 4.0) software. Timing sequences and data acquisition parameters were also

controlled from the XMASS software.

Method Fundamentals

ESI/MS

The electrospray process can be summarized in several steps. 1) The solution is

dispersed as a spray of charged drops from a needle which is held at high electric

potential. 2) These drops shrink in size by repeated solvent evaporation and uneven drop

fission. 3) Individually charged ions are ejected from these drops and enter the mass

spectrometer. The steps of this process are each discussed in depth in the following

paragraphs. The electrolytic nature of ESI is also discussed along with two important

implications. 1) A charge balance is required in the needle and oxidative reactions must

occur to achieve it. 2) The oxidation process can be used to ionize neutral molecules.

Charged droplets are generated by spraying a solution from a needle that is typically

0.1 mm internal diameter or less. The needle is held at a high electric potential of 2-5 kV

relative to an oppositely charged plate, which is 1 to 3 mm away. Figure 3.3 shows a

schematic of how the ESI setup operates. In the positive ion mode, which is the

perspective used in this discussion, the needle is positively charged and the plate is held

at ground or a negative potential. Because of the small diameter at the tip of the needle, a

high electric field, E, is set up at this point. That field is given by the equation [Pfeifer *et
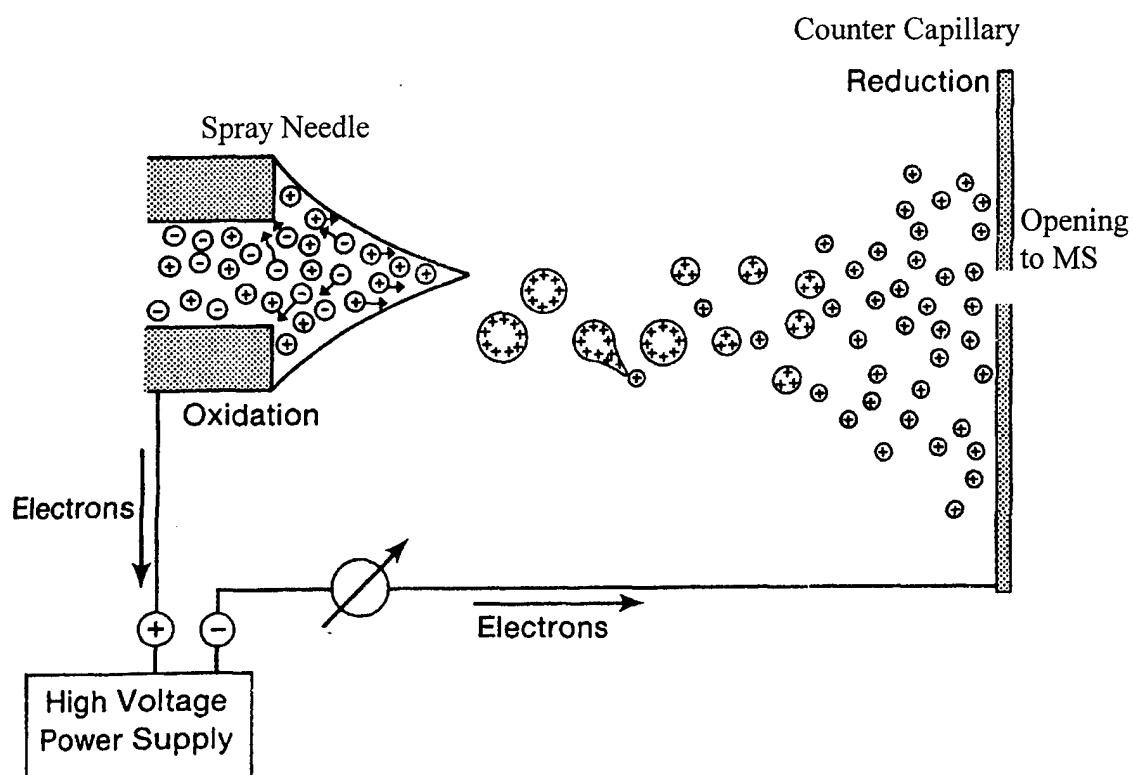
al.*, 1968]:

Figure 3.3. Schematic illustration of the ESI process. Adapted from Kebarle and Tang, [1993].

$$E = 2*V / [r * ln (4d/r)] \qquad\qquad (3.1)$$

where

> V = the applied voltage applied
> r = the radius of the needle
> d = the distance between the needle and the counter electrode

The electric field penetrates the solution at the needle tip and the ions in solution respond to counteract it. Positive ions are pushed out of the tip of the needle toward the surface of the liquid, and negative ions are drawn in to the solution and toward the needle itself. This electrophoretic migration, as it is termed, sets up a double layer in solution. An electrolyte is often added to the solution to make it conductive enough to form this double layer. The specific conductivity of the solution, σ_s, becomes the product of the limiting molar conductivity of the electrolye chosen, λ_m^0, and its concentration in the solution, C_E [Ganem et al., 1991].

$$\sigma_s = \lambda_m^0 C_E \qquad\qquad (3.2)$$

As the positive ions accumulate at the liquid meniscus, they repel each other and push out of the needle forming a cone of liquid known as the Taylor cone [Taylor, 1964]. If a high enough field is applied, the positive ions overcome the surface tension of the liquid and the Taylor cone will destabilize. Liquid droplets containing excess positive ions are expelled from the tip of the Taylor cone in a jet spray. The potential necessary to form this spray, V, depends on the viscosity of the solution, and is given by the relation [Loo et al., 1992]:

$$V = [2 \times 10^5](\gamma r)^{1/2} ln (4d/r) \qquad\qquad (3.3)$$

where

> 2×10^5 is a constant that comes from combining $cos\ \theta$ (the half angle of the Taylor cone) and ε_0 (the permittivity of vacuum)

γ = the viscosity of the solution
r = the radius of the needle
d = the distance from the opposing plate

After the charged droplets are expelled, they begin to shrink in size. There are two mechanisms by which this occurs. The first is the evaporation of solvent molecules from the drop driven by the absorption of thermal energy. The second process is uneven drop fission. As solvent molecules evaporate, the radius of the drop shrinks, and the ion-ion repulsions within the drop increase. These repulsive forces increase until they overcome the surface tension of the drop. At this point up to 20 smaller drops are expelled from the parent droplet, in a manner very similar to the original jet spray from the Taylor cone as shown in Figure 3.4. Since the offspring droplets are formed from the drop's surface where the positive ions have migrated, up to 15% of the parent drop's charge is carried away, but only 2% of its mass. The offspring drops are very close to the instability limit when they are formed. Both the offspring drops and the parent drop continue to lose solvent due to evaporation, both reach the point of uneven fission again, and the process repeats, creating ever smaller droplets.

Two theories have been put forth to explain the exact process of desolvating individual ions. Dole *et al.* initially proposed that the evaporation/fission process continues until drops reach a size where only one ion remains in the drop. As the rest of the solvent evaporates, this ion is left in the gas phase [Dole *et al.*, 1968]. This was called the charge residue model. Alternately, Iribarne and Thompson proposed that after the drop radius decreases to a certain size, individual ions are emitted from the surface of the drop instead of fission occuring. [Iribarne and Thompson, 1976; Thompson and Iribarne, 1979]. They called this the ion evaporation model. In depth experiments have failed to
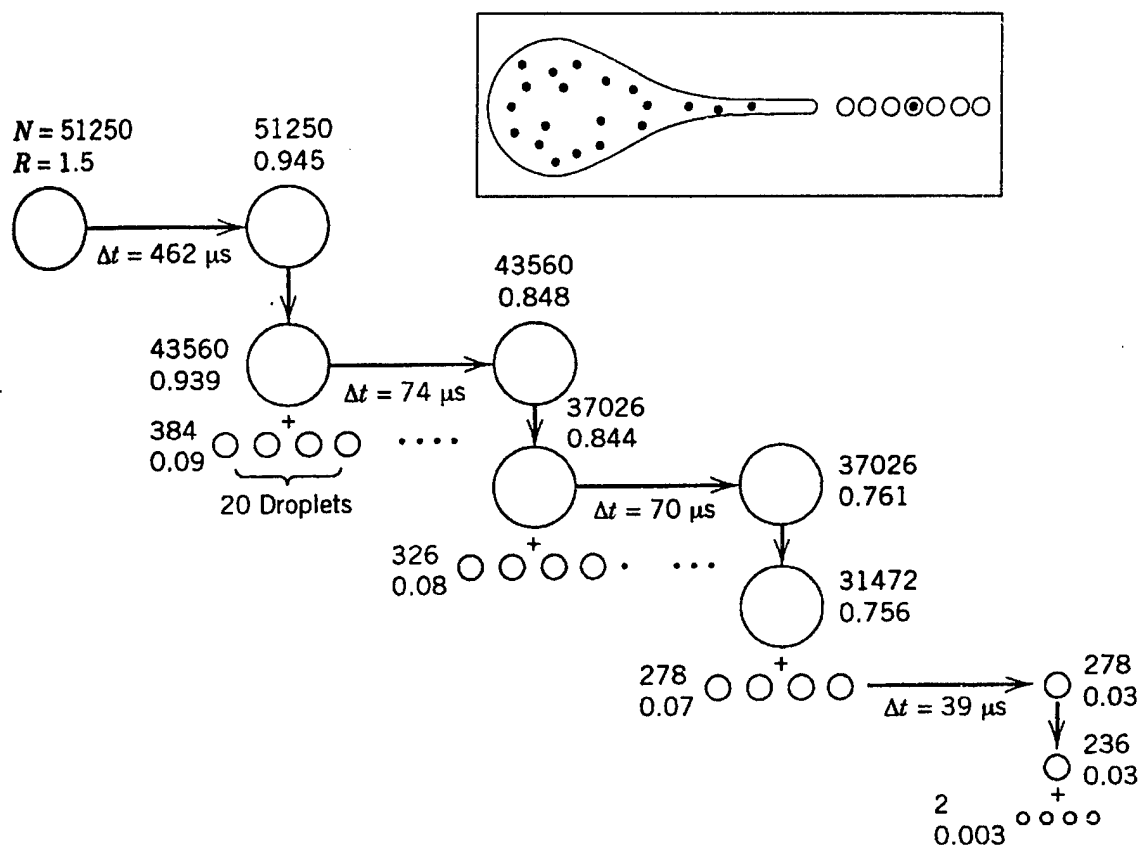
34

Figure 3.4. Schematic illustration of ESI droplet evaporation. Inset shows one droplet going through the uneven droplet-jet fission process. N= the number of charges in droplet. R = droplet radius in micrometers. Adapted from Kebarle and Tang, [1993].

differentiate between the two models, but in the end the result is the same. Gas phase ions are released from solution with a minimum of energy input. These free ions travel from atmospheric pressure through an orifice into the vacuum of the mass spectrometer. Excess solvent and neutrals are pumped away by the mass spectrometer's vacuum system, while positive ions are guided to the mass analyzer by ion optics.

The positive charge that is sprayed from the needle of the electrospray can be measured as the electrospray current, i_{ES}. An equation to characterize this current [Kebarle and Tang, 1993] shows the dependence of the ESI process on a number of variables:

$$i_{ES} = H \, \upsilon_f^{u} \, \sigma_s^{n} \, E_{ES}^{e} \qquad\qquad (3.4)$$

where
    H = a constant derived from the solvent's dielectric constant and surface tension
    υ_f = the solution flow rate
    σ_s = the specific conductivity of solution, calculated by Equation 3.2
    E_{ES} = the electric field imposed on the needle, calculated by Equation 3.1
    u, n and e are exponents that depend on values of the experimental parameters.

This equation is useful for optimizing the operation of the ESI nozzle. However, the fact that an ion current is generated in this process, as given by the equation, leads to an even more important conclusion. The electrospray nozzle is operating as a type of electrochemical cell.

As the positive ions leave the solution in droplets, they leave behind an excess of negative charge in the solution. This negative charge will build to oppose the applied electric field, eventually stopping the flow of ions if no other changes occur. However, if the excess negative charge can be removed, the electrospray will operate in a steady manner. To accomplish this, the electrospray is set up as a special kind of electrolytic cell.

To form this cell, the needle is connected to the opposing plate through the high voltage source. The needle acts as the anode, and redox active species in solution are oxidized as they contact the needle. The electrons which are transferred to the anode flow through the voltage source to the negatively charged plate, which acts as the cathode. The circuit is completed when positive ions and/or neutrals from the spray collide with the opposing plate and are reduced.

The implication of this setup is that there must be a charge balance between the positive charge that leaves the solution and the charge that is generated in solution. Stated another way, the ES current, i_{ES}, due to ions leaving solution must be equal to the current at the anode, i_F. The following expression applies [Cole, 1997]:

$$i_{ES} = i_F = \Sigma_j \, n_j \, A_j \, F \, v_f \qquad\qquad (3.5)$$

where

> n_j = the number of electrons involved in the oxidation of a mole of j
> A_j = Concentration of species j oxidized/reduced
> F = Faraday constant (9.648×10^4 C/mol)
> v_f = solution flow rate through the ES capillary

The operation of this electrolytic cell requires that oxidation reactions must occur in the needle. These reactions can take several forms. 1) The metal of the needle itself can oxidize. This is generally undesirable because the metal ions generate chemical noise in the mass spectrum. 2) Negative ions, either analyte or electrolyte, can be oxidized to neutrals. Products of this reaction would not be detected in the mass spectrum. 3) Positive ions could be produced from neutral species. This could include the solvent or a neutral analyte. Several of these reactions are possible at once, but the reaction that predominates will be that of the redox couple with the lowest oxidation potential. Careful

choice of electrode material and solution components will allow control of which electrolytic reaction occurs.

The oxidation reactions which occur in the needle raise the possibility of using the ESI process to electrochemically ionize neutral analytes in solution [Van Berkel *et al.*, 1992]. Neutral compounds that can be electrochemically ionized have low oxidation potentials and characteristics that aid in the stabilization of the positive ion formed. These compounds are usually aromatic, highly conjugated systems which can easily lose electrons from the π bonds; or they may contain heteroatoms, which have lone pair electrons to donate, or other electron donating groups. The molecular species most often produced in such electrochemical ionizations is the radical cation, M^{+} (due to the loss of an electron) instead of the protonated $(M+H)^{+}$ species.

There are several important considerations to be made when attempting electrochemical ionization. For any solution, the i_{ES} must be high enough to oxidize everything with a lower oxidation potential than the target analyte. Judicious choices in the composition of the solution can be made to eliminate lower potential species from solution. However, as seen in Equation 3.4, the solution composition also affects the functioning of the electrospray. Composition choices must not interfere with the production of the gas-phase ions. Therefore, the choice of solution components becomes a crucial balancing act.

FTICR-MS

The FTICR mass spectrometer is used as a sensitive detector in order to observe adducts formed in solution in EC/ESI. All mass spectrometers detect ions based on their mass-to-charge ratio (*m/z*). FTICR mass spectrometry uses the motion of an ion trapped

in a high magnetic field to detect the *m/z* of the ion. An ion moving in a magnetic field is subject to the Lorentz force given by equation 3.6.

$$Force = mass \; x \; acceleration = m \; dv/dt = zv \; x \; B \qquad (3.6)$$

where

m is the mass of the ion,
z is the charge of the ion
and v is the velocity of the ion.

The direction of this force is perpendicular to the plane determined by the direction of the ion's motion and the direction of the magnetic field. If the ion maintains constant speed, its motion is bent into a circle perpendicular to the magnetic field direction as shown in Figure 3.5a. The angular frequency of the ion or "ion cyclotron frequency", ω_c ,is given by Equation 3.7 [Marshall *et al.* 1998].

$$\omega_c = zB \, / \, m \qquad (3.7)$$

Only the mass-to-charge ratio, *m/z*, and the strength of the magnetic field, *B*, determine the cyclotron frequency. Since *B* is fixed, ions of a given *m/z* all have the same characteristic ICR frequency that is used to detect specific ions.

Figure 3.2 shows a diagram of an FTICR mass spectrometer showing 3 regions. The ions are formed in the source region. High voltages are applied to the ion optics in order to transfer these ions through the magnetic fringe fields into the high magnetic field. The ion cyclotron resonance (ICR) cell is used to trap the ions in the high magnetic field so that they can be detected. The trapping of ions is accomplished by a combination of the ion cyclotron motion of the ions in the x and y direction, and voltages applied to the plates at the ends of the ICR cell in the z direction. The trapped ions exhibit their characteristic cyclotron motion in the center of the ICR cell. The orbits of ions of a
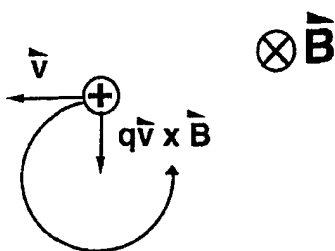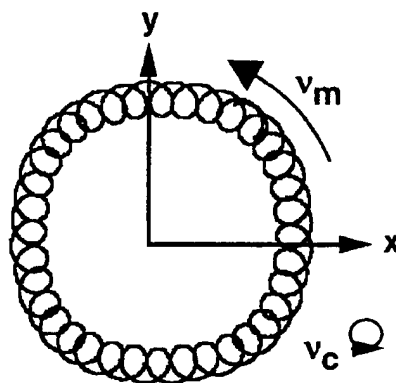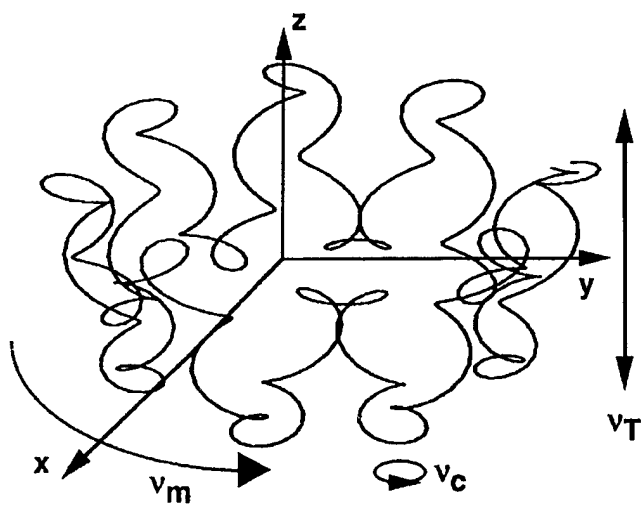
Figure 3.5. Ion motion in FTICR-MS. (a) cyclotron motion (b) magnetron motion (c) 3-D motion of trapped ion in ICR cell [Marshall *et al.*, 1998].

given *m/z* are out of phase, rendering them undetectable at this stage. Their orbital radius depends on their velocity in the xy plane, which is determined by their thermal energy when they enter the magnetic field.

To detect the ions, they must be coherently excited to a larger orbital radius. Ions of a specific *m/z* value can be selected and excited to a larger radius by applying a spatially uniform electric field to the ICR cell plates that oscillates at the cyclotron frequency of those particular ions, as shown in Figure 3.6a. As the ions absorb energy from this resonantly oscillating electric field, they are pushed outward in their orbit as a spatially coherent ion packet. The ions now exhibit what is known as magnetron motion in addition to their original cyclotron motion. The 2-D motion of an ion in the cell is shown in Figure 3.5b. The ions also oscillate in the z direction between the trapping plates of the cell. The addition of this motion gives a 3-D picture of the ions' motion inside the cell as shown in Figure 3.5c.

As this coherent ion packet alternately orbits past the two opposing detection plates as shown in Figure 3.6b, it induces an image current in these plates. This current is detected as the time-domain signal of the FTICR shown in Figure 3.7a. A frequency spectrum can be generated from the time-domain signal by applying a Fourier transform. This frequency spectrum is due to the frequency of the ion cyclotron motion, which is related by Equation 3.7 to the mass-to-charge ratio of the ions. A Fourier transform of the image current is shown in Figure 3.7b.

The minimum number of ions that can be detected in the ICR cell, *N*, depends on certain cell parameters and may be calculated using the following equation, which assumes a 1 second acquisition and a S/N ratio of 3/1[Marshall, *et al.*, 1998]:
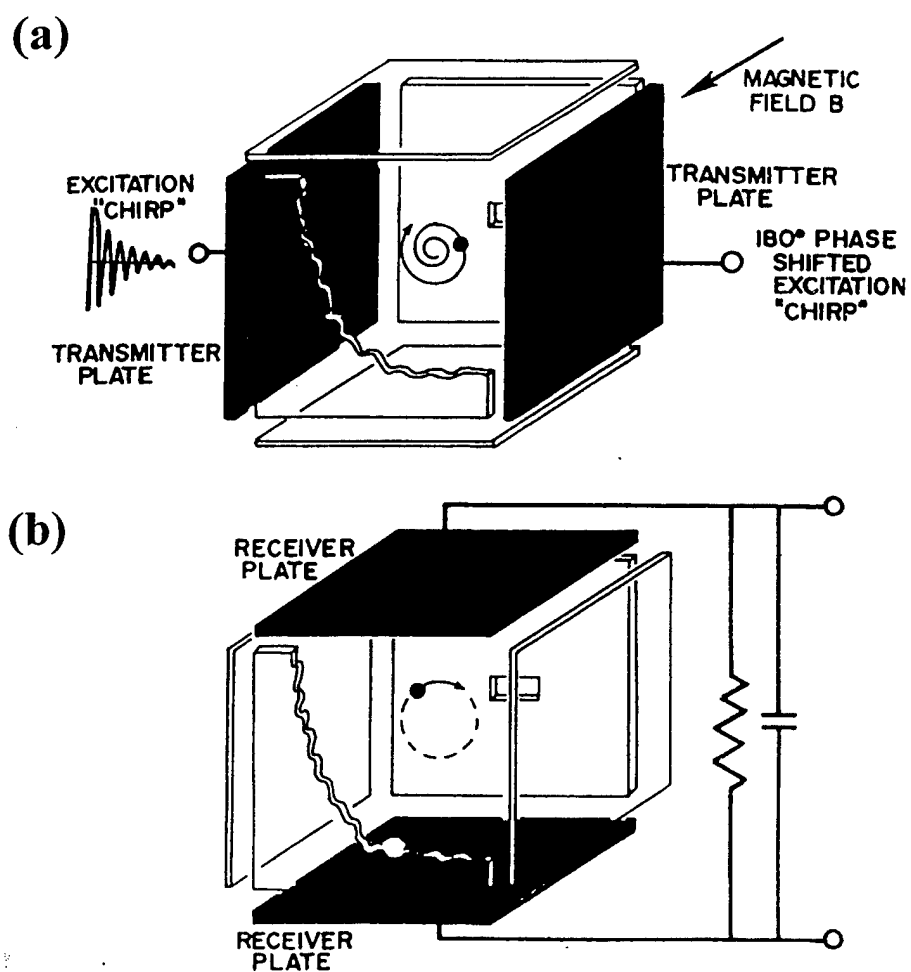
41

Figure 3.6. Functions of the FTICR-MS cell. (a) excitation (b) detection [Watson, ed., 1996].
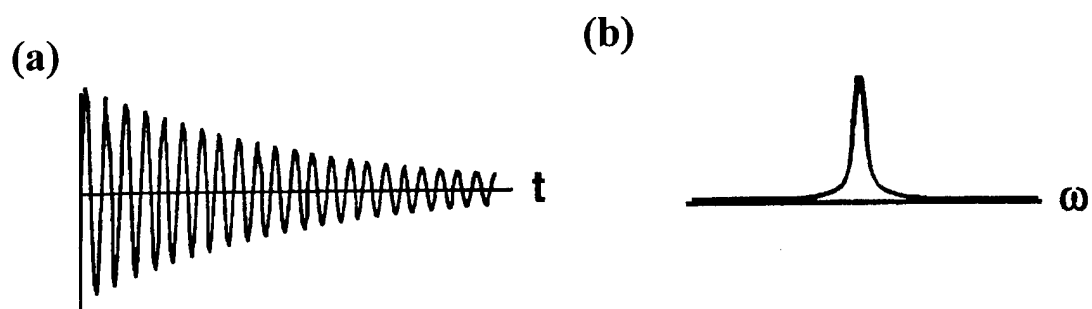
(a)

(b)

Figure 3.7. FTICR-MS signals. (a) time-domain transient (b) Fourier transform to frequency-domain [Marshal *et al.*, 1998].

$$N = CV / zA_{(r)} \qquad\qquad\qquad (3.8)$$

where

        C = the capacitance of the detection circuit with a typical value of 50 pF
        V = the amplitude of the detected voltage with a typical value of 3×10^{-7} V
        z = the charge of a single ion
        $A_{(r)}$ is proportional to the maximum allowable cyclotron radius

Using these typical values and assuming $A_{(r)}$ to be 0.5, approximately half of the maximum ion cyclotron radius, a theoretical detection limit of around 187 ions in the cell is found. This underscores the sensitivity of this detection method. This section on FTICR-MS is summarized from Marshall *et al.*, [1998] and Watson, [1997] and these works should be referenced for a deeper explanation.

Experimental Conditions

Reagents and Chemicals

HPLC-grade acetonitrile (MeCN), ACS certified methylene chloride (CH_2Cl_2), ACS certified pyridine, and reagent grade sulfuric acid (H_2SO_4) were obtained from Fisher (Pittsburgh, PA). Lithium trifluoromethanesulfonate, also known as lithium triflate, ($LiCF_3SO_3$) was purchased from Alfa Aesar (Ward Hill, MA). Anthracene and benzo[a]pyrene were obtained from Aldrich (Milwaulkee, WI). Guanosine and guanine were obtained from Sigma Chemical Co. (St. Louis, MI). All chemicals were used as received.

Solution Preparation

All sample solutions were prepared on the day they were run from stock solutions that were made in advance and refrigerated between uses. The following is a list of stock solutions that were prepared: anthracene (1×10^{-2} M) in methylene chloride, benzo[a]pyrene (1×10^{-3} M) in methylene chloride, lithium triflate (1×10^{-3} M) in

acetonitrile, guanine (1×10^{-2} M) in 2M sulfuric acid, guanosine (1×10^{-2} M) in 1×10^{-3} M sulfuric acid.

The PAH sample solutions were prepared in a mixed solvent system. PAHs are nonpolar compounds and require a nonpolar solvent, such as methylene chloride. The electrolyte compounds require a more polar solvent, such as acetonitrile, for sufficient solubility. Standard sample solutions were made to a solvent ratio of 50/50 v/v acetonitrile/methylene chloride. All sample solutions were made in a 1 mL volume. A Microsoft Excel spreadsheet was set up to calculate the volumes of each stock solution and solvent which should be added to give appropriate final concentrations in a 1 mL volume. When the nucleophiles pyridine, guanine, or guanosine were added to sample solution, the spreadsheet was recalculated incorporating the volume of the nucleophile solution into the final 1 mL solution volume.

Sample solutions were made by pipeting appropriate volumes into 1.5 or 2 mL plastic sample tubes with caps. Disposable plastic tips were used with microliter pipets to measure out volumes. Each tip was used for only one stock solution, for example, one tip for transferring anthracene stock solution. The reagents were added sequentially for each sample solution in this order: methylene chloride, PAH stock solution, acetonitrile, LiT stock solution, nucleophile solution. At the end of solution mixing, the tips were disposed. All solutions were made fresh the day they were used.

For the B[a]P-guanosine solutions, a new solvent ratio of 80% acetonitrile, 10% methylene chloride and 10% aqueous guanosine solution was used. The higher acetonitrile percentage allowed higher concentrations of the guanosine nucleophile to be added to solution without the solvents separating. This ratio did not work well with

anthracene because the concentration of water was so high that only water adducts were observed. B[a]P was less reactive toward water than anthracene, and could be used under these conditions.

Since B[a]P is a known carcinogen, and on the EPA's priority pollutant list, special care had to be taken when making solutions. The exposure route of concern for B[a]P is by direct contact with skin. Gloves and goggles were worn whenever mixing or working with B[a]P solutions and all mixing was performed in a fume hood. The concentration of B[a]P never exceeded 1 mM in any solution. Any excess solution not sprayed in the mass spectrometer was collected into a stoppered glass bottle and labeled as B[a]P waste. The syringe was rinsed with 1mL of methylene chloride into the waste bottle as well. Pipet tips and gloves were sealed in a plastic bag and disposed of after use. The mass spectrometer was baked out at 220 degrees Celsius at the end of the B[a]P experiments for a period of 6 hours.

EC/ESI-FTICR MS Conditions

In a typical sample run, the syringe, supply line, and EC cell were rinsed with 0.5 mL of both acetonitrile and methylene chloride to clear the previous sample from the system. (If nucleophiles had been added, a full cell regeneration, as described later, was performed to remove any nucleophile adsorbed to electrodes.) A sample volume of 250 μL was loaded into the syringe. A volume of 100 μL of this sample was pushed through the transfer lines after loading to clear them and bring the sample solution to the needle tip. Sample solutions were usually sprayed at a flow rate of 75 μL/h and at an ESI voltage of 3.3 kV. If the experiment were being run in the EC/ESI mode, then 5 Volts were applied across the EC cell electrodes. In the EC/ESI mode data were not taken until a

time period of 2 minutes had passed, to ensure that products of the EC cell had reached the ESI tip and were expressed in the mass spectrum.

The inlet to the mass spectrometer is through a stainless steel capillary that is 170 mm long with a 500 μm i.d. The capillary was heated to 120° C to facilitate sample desolvation. The end of the capillary was held at 100 V and the skimmer at 10 V for the electrolyte and limit of detection studies. The difference between these voltages pushes the ions from the atmospheric pressure region of the capillary into the vacuum region of the mass spectrometer. It was found that a capillary voltage of 80 V and skimmer voltage of 8 V worked better for the detection of adducts, and these values were used in the adduct studies.

The source region of the mass spectrometer was maintained at a pressure of 5.0×10^{-6} mbar by the two turbopumps. Once the ions enter the mass spectrometer they are accumulated in the hexapole. The hexapole offset voltage was set at 1.47 volts. A trapping voltage of 3.00 volts held the ions in the hexapole for a time period (d1) of 1 second. Then the extract voltage of 6.00 volts was applied to pull the ions out of the hexapole, sending them through the ion optics to the cell. The vacuum pressure in the cell was maintained at 4.3×10^{-10} mbar by two additional turbopumps.

Data Handling in FTICR MS

The Bruker Apex FTICR XMASS (version 4.0) program was used for the acquisition and processing of all recorded mass spectra. Data were collected over a mass range of 75 to 600 amu in the broadband detection mode. Twenty scans were recorded and averaged (unless otherwise specified) using 64K data points. Mass peaks were identified using the

"pick peak" command and absolute ion signal strengths were determined using the "report" function.

Regeneration of the EC Cell for EC/ESI-MS

Zhang reported a deterioration of the EC cell's performance after several hours of run time due to electrode oxidation and adsorption of the analyte and other contaminants. [Zhang, 2001] The cell regeneration scheme found in his dissertation was followed in a modified format at the end of each day. The cell was first flushed with 1 mL volume of methylene chloride to remove nonpolar compounds. Then 1 mL volumes of acetonitrile, acetone, methanol, and finally water were used to dissolve salts and polar compounds. A 2 M H_2SO_4 solution was loaded into the cell and allowed to remain for ten minutes to remove the oxide film from the electrode surface, after which time it was flushed with 1 mL volume of 2 M H_2SO_4. Finally, the cell was restored to its original condition by rinsing sequentially with 1 mL each of water, methanol, acetone, and acetonitrile.

CHAPTER 4
RESULTS AND DISCUSSION

In this study, a model PAH was chosen, electrochemically oxidized in an EC/ESI cell, and reacted with nucleophiles in solution. The reaction products were studied using FTICR-MS. The research was first focused on characterizing the response of the system to both the electrochemical cell voltage and to solution composition. The second focus of the research was to maximize the detection of PAH reaction products by optimizing a set of experimental operating parameters. A final goal was to detect a PAH-DNA adduct that had been generated in the electrochemical cell. Biological nucleophiles were added to PAH solutions and adducts sought in online detection. A benzo[a]pyrene-guanosine adduct that had been previously reported as being generated by electrochemical oxidation was detected at low levels.

EC/ESI-MS of Anthracene

Oxidation Pathway of Anthracene

Anthracene was chosen as a model PAH for this study because its electrochemical oxidation in acetonitrile has been well characterized in the literature [Majeski, 1968] and it is not suspected to be carcinogenic. Anthracene has two identical reactive centers, which makes identifying reaction products straightforward. The detection of anthracene cation radicals produced in ESI-MS was first reported by Van Berkel et al., [1992]. The EC/ESI-MS of anthracene has also been studied by Palii and Zhang [Palii et al., 2001, Zhang et al., 2002]. They have found that the cation radicals of anthracene react readily in solution and generate mass peaks for anthracene-water adducts. A reaction sequence

48

for the oxidation of anthracene by EC/ESI-MS was determined [Palii *et al.*, 2001] and is shown in Figure 4.1. Peover and White, [1967] proposed that the oxidation of anthracene follows an ECE scheme. The process begins with the removal of one electron from the π bond system, giving a radical cation at m/z 178. This cation is highly reactive, with a lifetime of only a few milliseconds [Peover and White, 1967] before a follow-up reaction occurs.

The nucleophilic addition of water to the radical cation produces a water adduct with a mass of 195. If this adduct is then oxidized, it generates the peak seen at *m/z* 195. However, a loss of hydrogen followed by electrochemical oxidation may also occur, generating 9-hydroxyanthracene at *m/z* 194. A loss of two hydrogens followed by oxidation gives 9-anthrone at *m/z* 193. A second addition of water is also possible at the 10 carbon of anthracene; the final product in this pathway is anthraquinone. Majeski *et al.* reports that this is the major product of complete electrolysis of anthracene in acetronitrile when water is present in high concentration [Majeski *et al.*, 1968]. An intermediate ion in the pathway to anthraquinone is observed in the mass spectrum at *m/z* 211. A representative mass spectrum taken with the EC cell voltage off is shown in Figure 4.2. It shows peaks due to the radical cation, the mono-oxygenated intermediates, and the di-oxygenated intermediate.

Effect of EC/ESI-MS on Ion Signal

Applying a voltage across the electrodes of the electrochemical cell oxidizes the analyte in solution before it reaches the needle tip, often enhancing detection [Bond *et al.*, 1995; Zhou and Van Berkel, 1995]. Figure 4.3 demonstrates at least a factor of 2 increase observed in the signals due to anthracene and its adducts by applying 5 Volts to
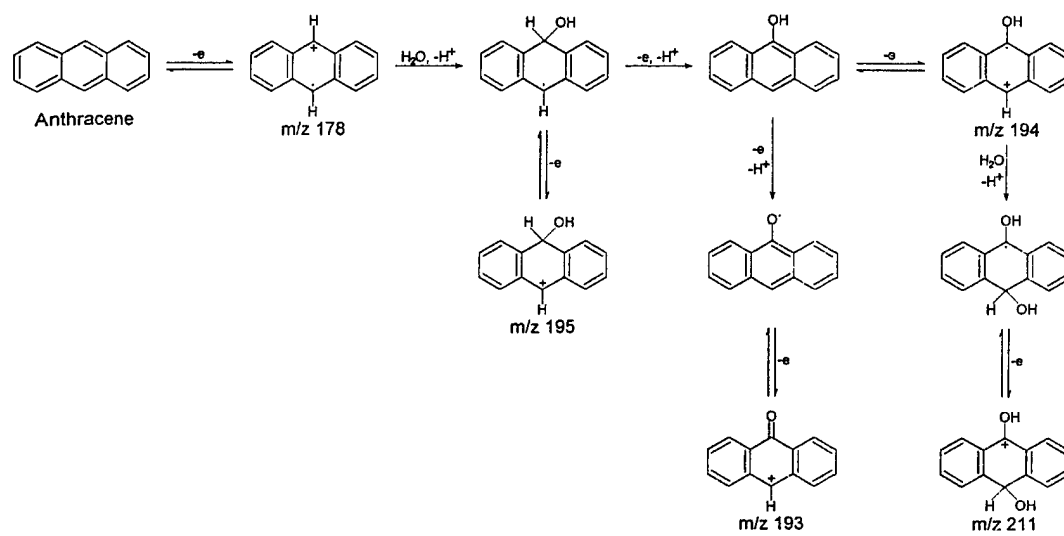
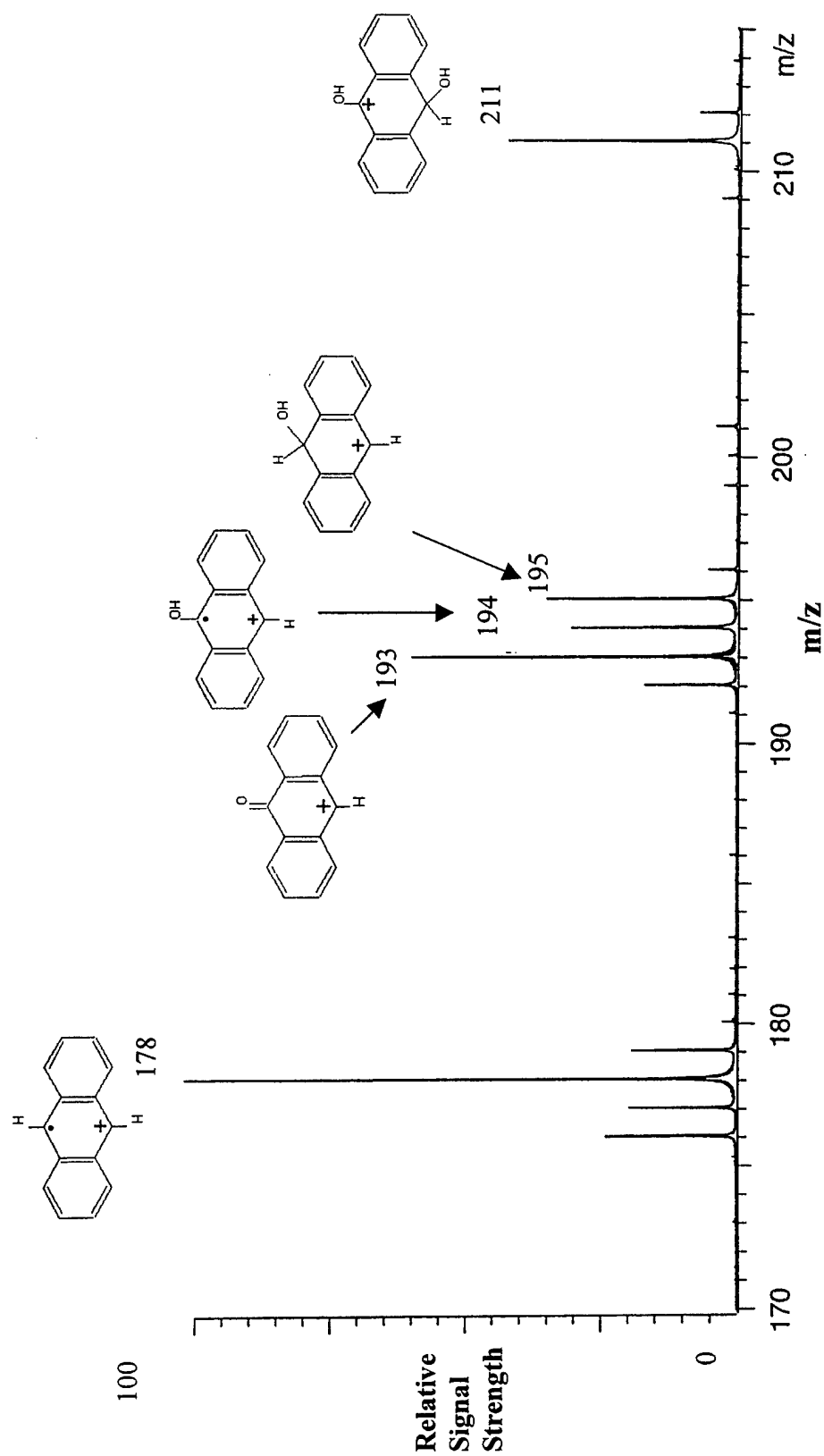**Figure 4.1.** Anthracene reaction pathway [Palii *et al.*, 2001].

Figure 4.2. Hydrolysis of anthracene radical cation in ESI-MS.
Conditions: 1mM anthracene, 250 µM LiT in 50/50 v/v ACN/MeCl$_2$
Flow rate: 75 µL/h, ESI voltage: 3.3 kV, Capillary voltage: 100 V.
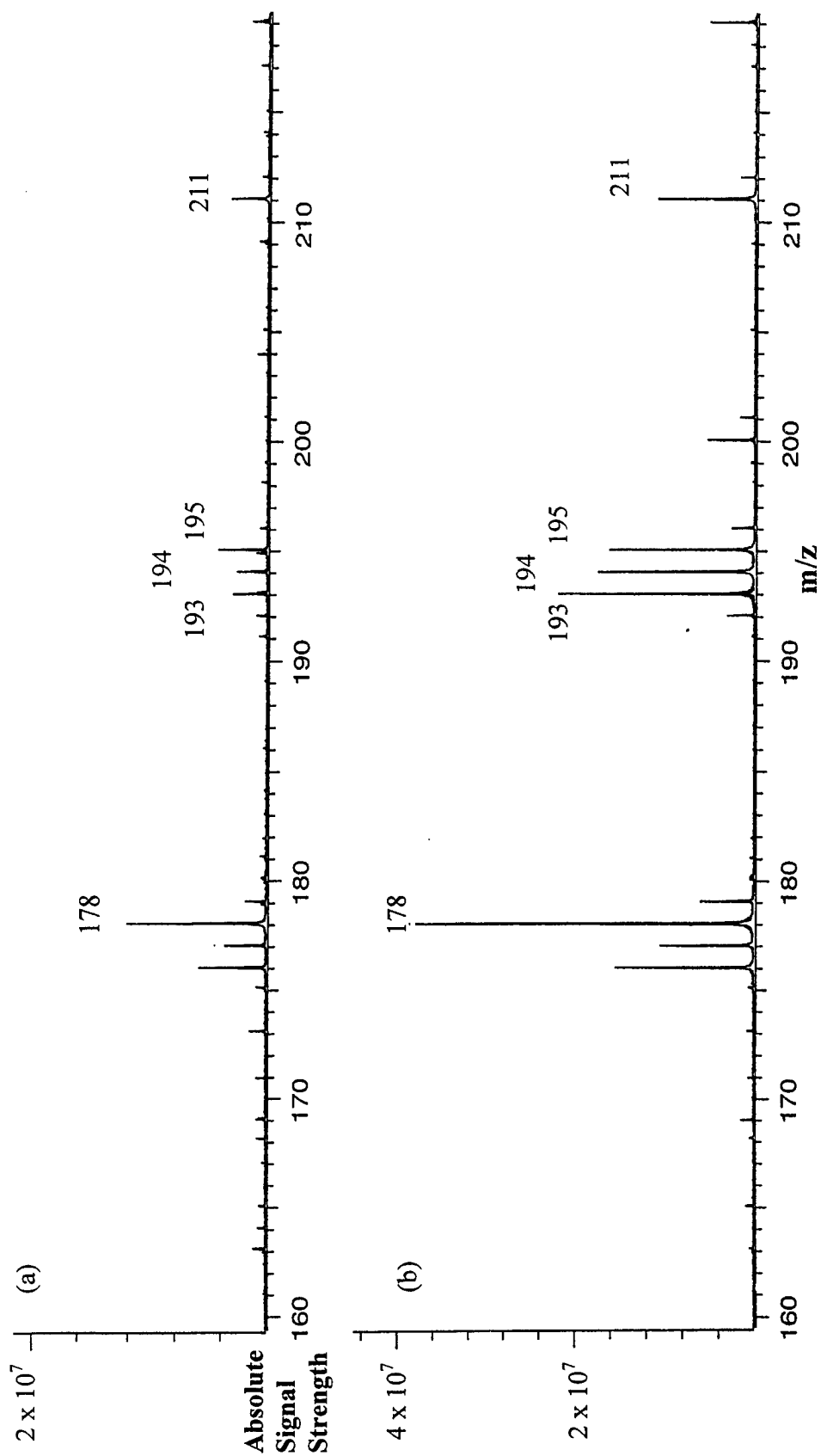
Figure 4.3. Singnal strength increase in anthracene spectrum (a) ESI-MS (b) EC/ESI-MS. Conditions: 100 µM anthracene, 250 µM LiT in 50/50 v/v ACN/MeCl$_2$ Flow rate: 75 µL/h, ESI voltage: 3.3 kV, Capillary voltage: 100 V, EC cell on: 5.0V.

the EC cell. In ESI, water adducts are detected when anthracene is oxidized in the needle tip and reacts with water before it is liberated into the gas phase. The time for reaction with water is limited. However, anthracene radicals are highly reactive and water adducts are readily observed in the mass spectrum. When the electrochemical cell is on, anthracene is oxidized long before it reaches the spray. The radical cations that are generated have a greatly increased chance to react with water in the solution. These adducts are easily oxidized as they are sprayed from the ESI needle and are detected in much higher numbers.

The increased reaction time PAH radical cations have when generated in the EC cell should be beneficial in detecting PAH adducts with other nucleophiles as well. Biological nucleophile adducts may be observed only if they have a long time for interaction with the radical cations. For long interaction times to be possible, the radical cations must be stable in solution. If the solvent or other contaminants in the system are more reactive toward the radical cations and are present in higher concentrations, they may consume all the PAH radical cations before any can react with biological nucleophiles. For this reason it is important to choose a solvent system that stabilizes the radical cations once they are formed. We might also conclude that PAH-DNA adducts would be easier to detect for PAHs that have cation radicals that are intermediate in their stability. Highly reactive radical cations like anthracene might be too quickly consumed, and highly stable radical cations might not react at all.

Effect of Cell Voltage on Ion Signal

The voltage that is applied to the EC cell determines the electrochemical reaction that occurs and the types of ions that are produced [Zhou and Van Berkel, 1995]. To test how our cell voltage affects the ion signal, the voltage applied to the EC cell was increased

from 1 V to 7 V in 1 V increments. The strength of the radical cation (m/z 178), mono-oxygenated water adducts (m/z 193,194,195) and di-oxygenated water adduct (m/z 211) ion signals is plotted at each voltage in Figure 4.4. The electrochemical oxidation potential of anthracene in acetonitrile with 0.1 M silver perchlorate and 0.5 M sodium perchlorate as electrolyte is reported to be 0.88V [Majeski, 1968]. As the cell voltage nears the anodic peak potential, we would expect to see the water adduct signals increasing steadily. Past this voltage we would expect a plateau to be reached in signal strength. In Figure 4.4, a slow increase is observed in adduct signal enhancement beginning at 2 V and increasing to 6 V where the signal reaches a plateau.. The higher voltages required to generate signal enhancement in our system can be attributed to the iR drop in solution which makes the actual electrode potential lower than the applied potential [Zhou and Van Berkel, 1995].

Effect of electrolyte concentration

The need for electrolyte in the operation of EC/ESI-MS and the potential drawbacks of high concentrations of electrolyte were discussed in some detail in Chapter 2. In the following experiment, an optimum electrolye concentration was determined for our system in both the EC cell on and cell off modes. Lithium trifluoromethanesulfonate (lithium triflate or LiT) was chosen as an electrolyte to limit suppression effects. The concentration of anthracene was kept constant while the electrolyte concentration was varied over a range from 10 μM to 1mM. The total signal of the anthracene radical cation and water adduct ions was plotted against LiT concentration in both the cell on and the cell off operating modes, and that graph is shown in Figure 4.5. The ESI current was recorded and each run and is shown on a separate scale in Figure 4.5. The resulting
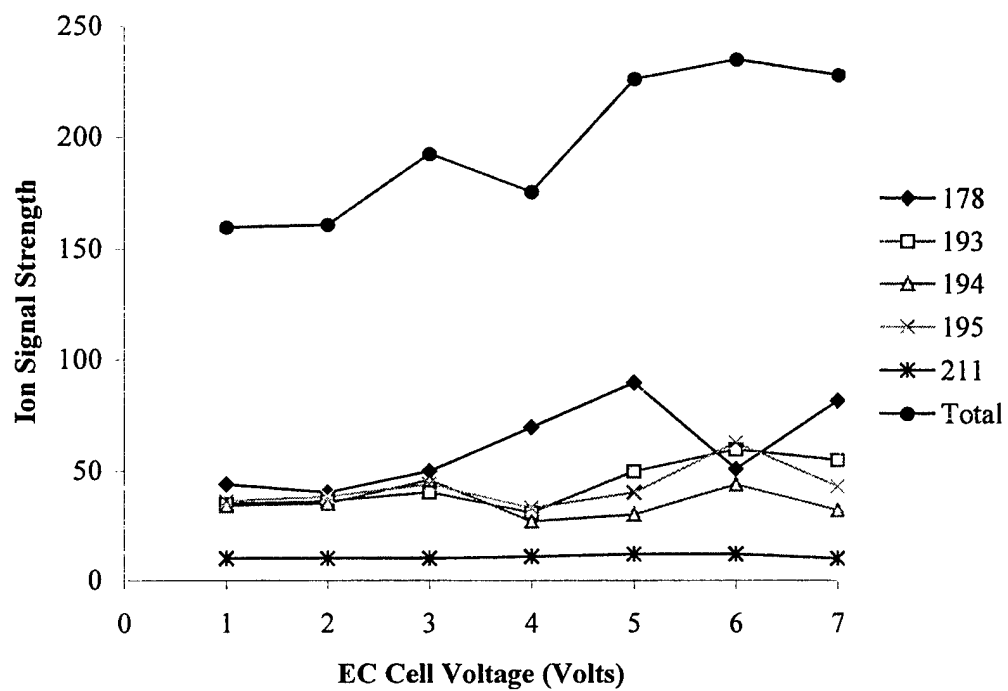
Figure 4.4. Ion signal strength with EC cell voltage.

curves show a maximum signal at an electrolyte concentration of 500 µM LiT in the cell off mode.

The ratio of analyte to electrolyte in this case is at 2:1. The taper of the signal at higher concentrations is likely due to suppression effects as the electrolyte concentration approaches that of the analyte. Signal strength drops at lower concentrations because the conductivity of the solution is falling, and i_{ES}, the ESI current, is dropping. As i_{ES} drops, so must the Faradaic current in the ESI needle, which means less anthracene will be oxidized.

In the cell on mode, the entire signal curve is shifted to lower LiT concentrations, and the maximum is found at 250 µM LiT. Comparing the ESI current for the two cases shows that the cell on current is twice as high as the cell off current, even when the signal intensities are similar. For the i_{ES} current to increase, more ions must be sprayed from the needle tip. These ions likely come from two sources: 1) they are generated in the EC cell as stable ions that persist until they are sprayed and 2) the EC cell generates products which are more easily ionized in the tip of the ESI needle. This increase in ions in solution appears to cause more signal suppression than ESI alone at higher electrolyte levels, but at lower electrolyte levels the analyte signal is double that of the ESI signal as seen from Figure 4.5. The conclusion reached was that the EC/ESI technique is a more efficient ionization source at low electrolyte levels.

Effect of Analyte Concentration

A limit of detection experiment was performed next, in which the analyte concentration was decreased while the electrolyte was held constant at 250 µM LiT. This electrolyte value was used because it gave the highest signals in the EC/ESI mode of the
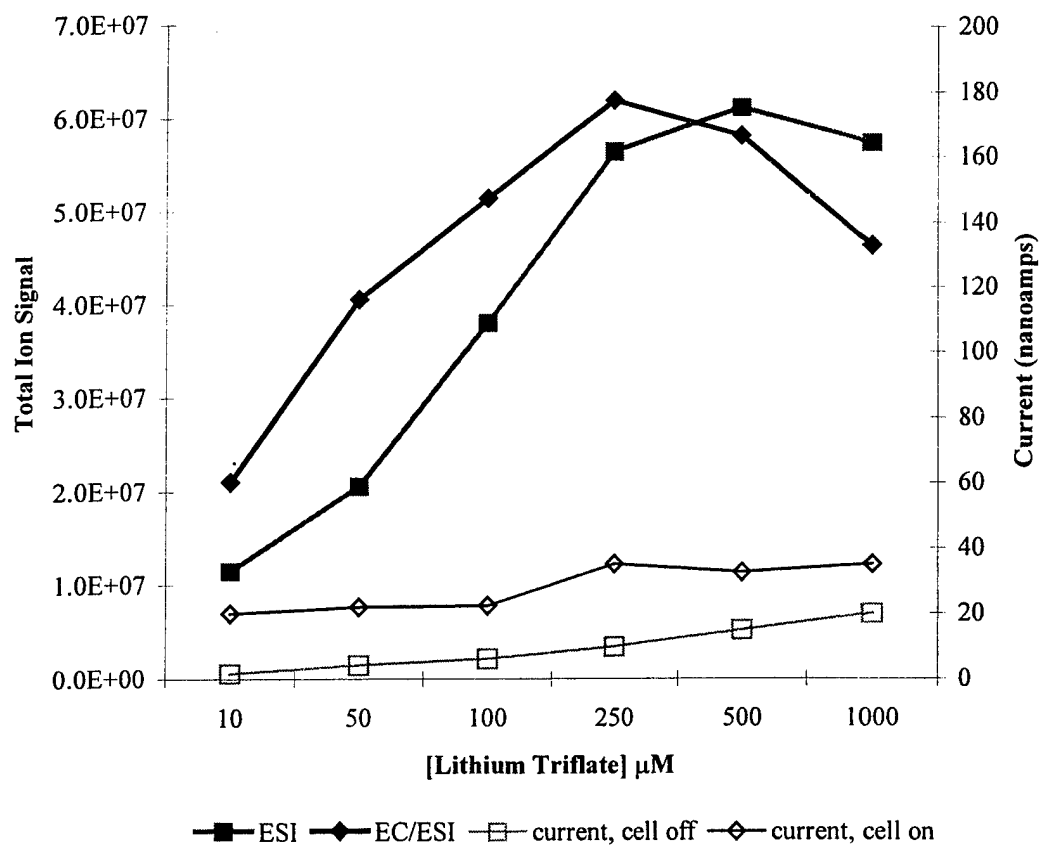
Figure 4.5. Ion signal strength with electrolyte concentration.

experiment. The cell was again operated in both the cell on and cell off modes, and the total ion signal strengths plotted against the anthracene concentration. The resulting graph is shown in Figure 4.6. The limit of detection in the cell off mode was 10 μM. The cell on curve demonstrated higher ion signals at all analyte concentration values, including a lower limit of detection of 5 μM. The EC/ESI operation of the device overall has lower detection limits. Zhang [2001] reported similar results for anthracene; however, he achieved a lower detection limit of 1μM in the cell on mode. This greater sensitivity is likely due to the increased ionization efficiency from using a 100 μm i.d. ESI needle as opposed to the 200 μm i.d. ESI needle used in this experiment.

A second experiment was performed in which the ratio of analyte to electrolyte was held at a constant ratio of 2:1. In this case, the limit of detection displayed was only 50 μM. It was observed that the ESI current dropped rapidly as the analyte/electrolyte concentration decreased. I concluded that the ESI current was no longer high enough to effect sufficient oxidation of anthracene for its detection. Operation with 250 μM of lithium triflate provides the best signal case.

Optimization for Detection of Reaction Products

I was interested in using EC/ESI-MS to detect nucleophilic reactions which occur in solution after the oxidation of PAH compounds. It has been demonstated by many authors [Zhang, 2001; Zhou and Van Berkel,1995; Xu *et al.*, 1996] that the parameters which control the ESI process affect the signal which is produced in the mass spectrometer. Several important ESI parameters have been chosen to study their influence on the detection of nucleophilic reaction products. These studies were carried out using solutions composed of 1mM anthracene and 250 μM LiT in 50/50 v/v acetronitrile and
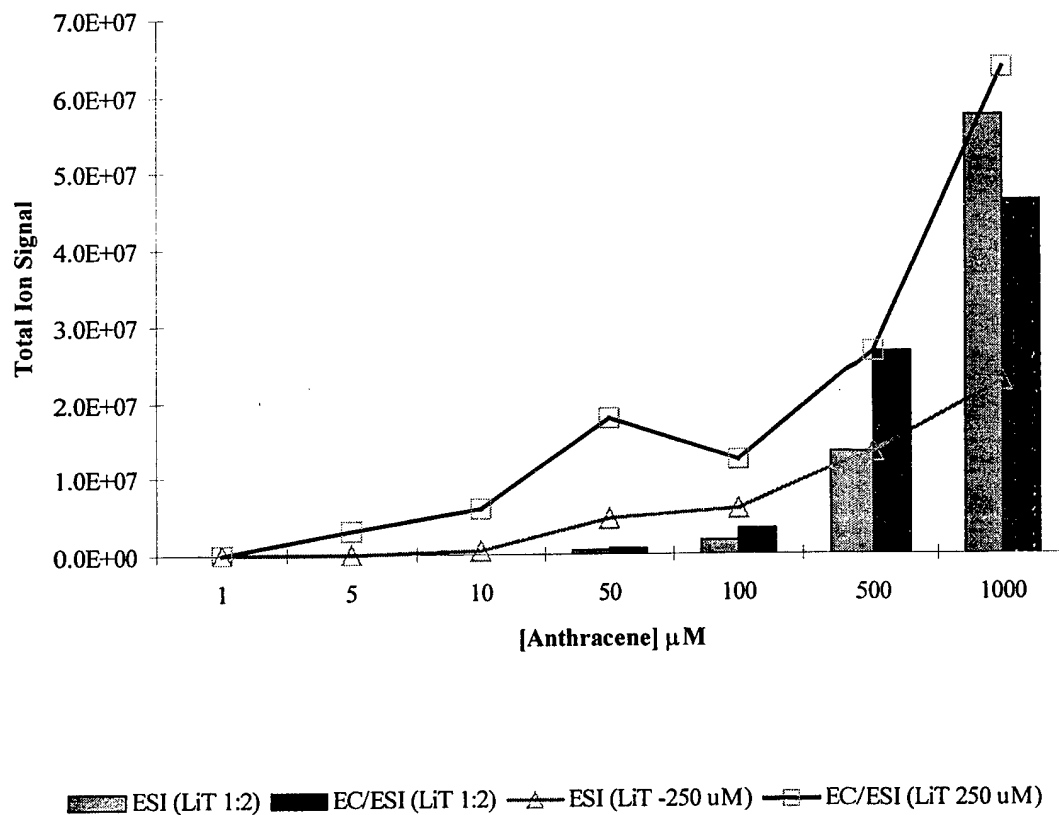
Figure 4.6. Comparing the limit of detection with two electrolyte schemes.

methylene chloride. This composition was chosen because it generated the highest adduct signal in the previous experiments under cell on conditions.

The nucleophilic reaction that is monitored is the reaction of the anthracene cation radical with water. Water is a strong nucleophile [Xu et al., 1996] and is very difficult to eliminate from solution. It has been estimated that even in dry solvents, water exists at concentrations of 4-10 mM [Majeski, 1968], which is higher than the concentration of the anthracene in solution. I was also spraying the solution into ambient atmospheric conditions, in which high concentrations of water vapor are present. The water reaction, then, is unavoidable and makes a convenient diagnostic to see how electrospray parameters are affecting nucleophilic reactions.

To determine the effect of the instrumental parameters, these parameters were varied over a suitable range and the intensities of the radical cation at m/z 178, the mono-oxygenated adducts at m/z 193, 195, and 195, and the di-oxygenated adduct at m/z 211 were monitored. The signal strengths of the mono-oxygenated peaks are summed in each graph since they all result from one nucleophilic reaction. All five ions are summed to give the total ion intensity for each case. The experimental parameters were set as follows, with the exception of the parameter that was being varied in each case: a flow rate of 75 µL/hour, a needle voltage of 3.3 kV, a capillary voltage of 100 V, and a hexapole collection time of 1 second. The EC cell was off for this experiment set.

Flow Rate

The first parameter investigated was the flow rate of the solution. This parameter is bounded by the stability of the electrospray. I use the ESI current reading to determine if a steady spray is being formed. The ESI current was stable when operated between 45

μL/h and 120 μL/h for our system. A graph of the ion signal strengths is shown in Figure 4.7. The total ion signal was much greater at low flow rates and declined steadily as the flow rate increased. I attributed this trend to the increased time the analyte spends in the oxidizing environment of the needle at lower flow rates [Zhou and Van Berkel, 1995]. The water adduct is the base peak at the lower flow rates, and also steadily diminishes as higher flow rates are reached. This suggests that low flow rates would be a better operation region for the detection of adduct species.

Needle Voltage

A second parameter explored was the high voltage applied to the electrospray needle. The range of needle voltages available begins with the electrospray onset voltage and ends at the voltage where the spray again destabilizes. In this setup the onset value was 2400 V and the stable range ended at 3600 V. A curve was generated at 200 V increments and is shown in Figure 4.8. The total ion current was greatest at the onset voltage, reached a secondary maximum at 3200 volts, and then decreased rapidly. Overall, the secondary maximum at 3200 demonstrated the highest anthracene adduct signal. Higher voltages may help to increase oxidation further downstream in the needle, giving radical cations more time to react and adducts that are produced more time to be oxidized before they are sprayed. However it appears that if ESI voltage is too high then ESI current becomes unstable and oxidation is less efficient. An operating condition of 3200 volts was chosen for future adduct studies.

Capillary Voltage

The desolvating capillary voltage has a large effect on the mass spectra of anthracene, although it does not relate to the solution phase chemistry. As the electrospray droplets travel through the capillary, ions are desolvated by absorbing
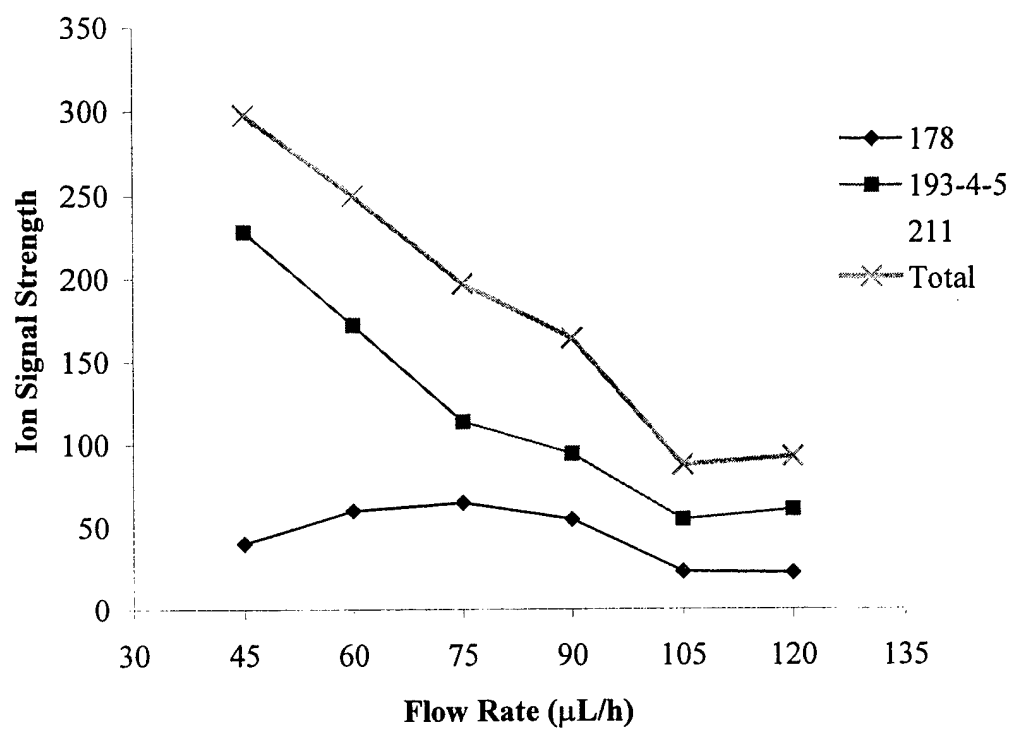
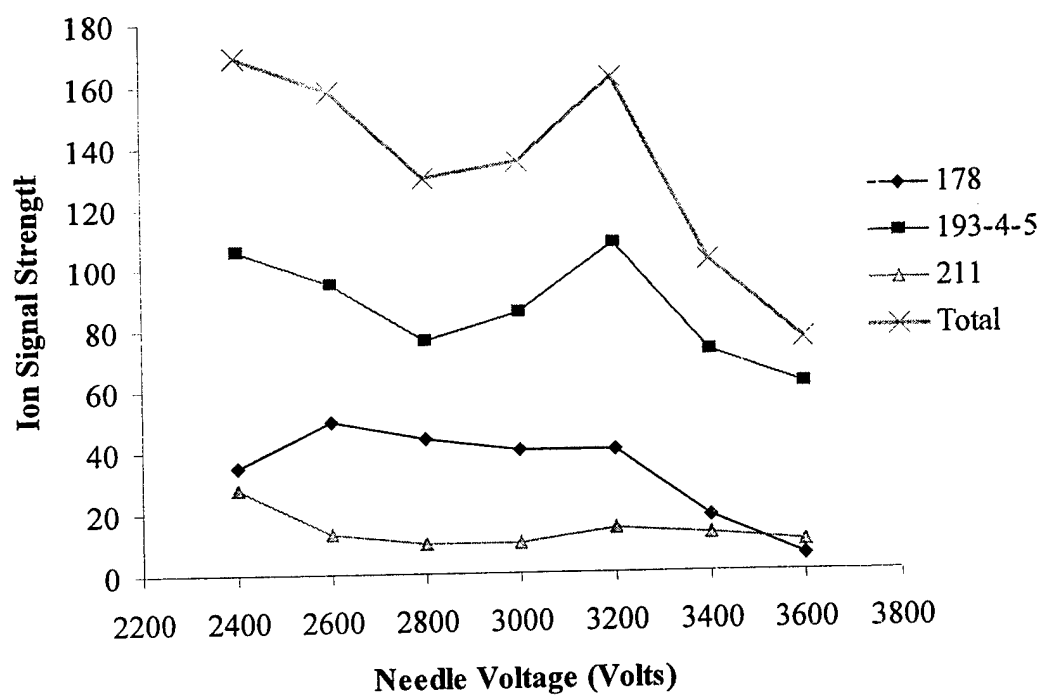**Figure 4.7.** Ion signal strength with flow rate.

Figure 4.8. Ion signal strength with needle voltage.

thermal energy. Once they reach the end of the capillary, the uncharged solvent is pumped away, and the charged ions enter the mass spectrometer. The difference between the capillary and skimmer voltages is what pushes the desolvated ions from the end of the capillary region into the high vacuum region of the mass spectrometer. As the ions are accelerated by the applied potential, they can undergo collisions with evaporated solvent molecules and atmospheric gases. Gas phase collisions can result in reactions that form new adducts or cause the dissociation of adducts formed in solution. The frequency and outcome of these gas-phase reactions can significantly change the mass spectra that are observed.

In a test of this effect, the capillary voltage was varied from 20 to 200 V in increments of 20 V, with the skimmer fixed at 10 V. The experimental results are shown in Figure 4.9. Below 20 volts signal levels are buried in the noise because ions are not transferred efficiently and above 200 V all ion signals decrease rapidly due to energetic collisions. Total ion signal strength reached a maximum at 100 V. At the lowest capillary voltage, the radical cation is the base peak. As the voltage increases between 60 and 100 V, the mono-oxygenated adducts increase and overtake the decaying radical cation peak. Two effects may be contributing here. The first is increased transfer efficiency of the higher mass adducts at higher capillary-skimmer potential differences. The second is the increased occurrence of gas-phase reactions of cation radicals with water molecules. Beginning at 100 V, I see a shift to lower mass mono-oxygenated adducts due to the loss of hydrogen, which is likely due to collisional dissociation of higher mass water adducts. Past 100 V, the water adduct signals decrease, and the radical cation begins to grow again. This could be evidence of collisional dissociation of water adducts yielding the
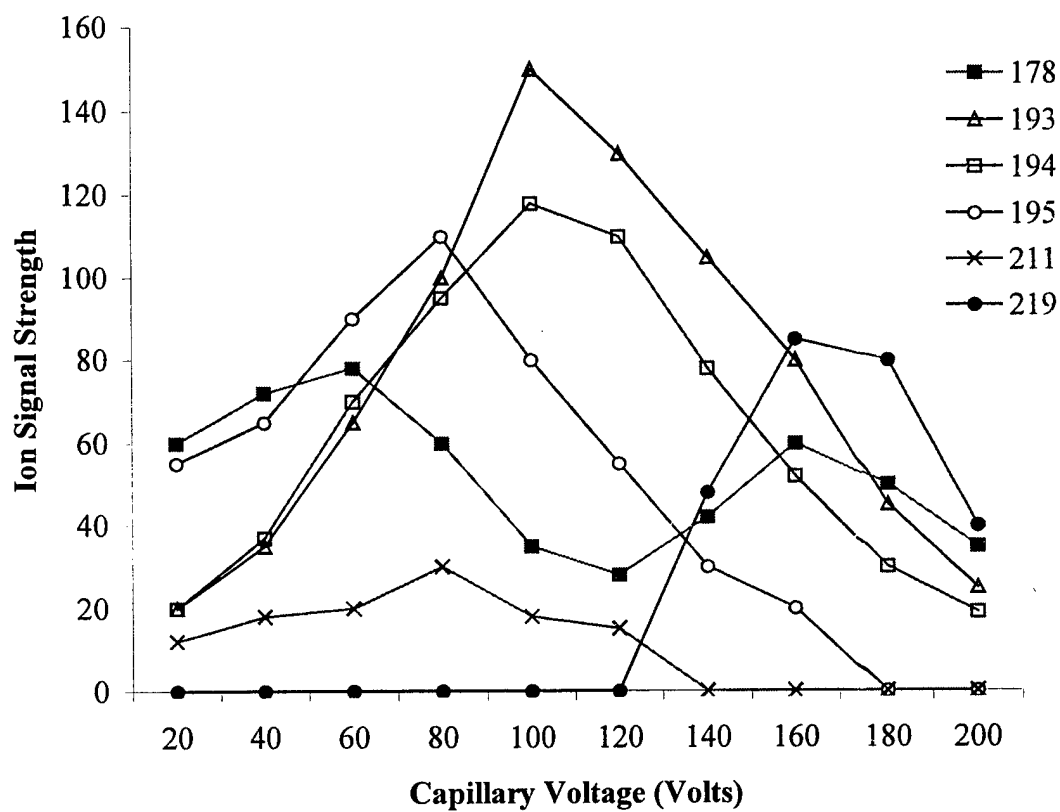
Figure 4.9. Ion signal strength with capillary voltage.

original cation. I also see the rapid growth of the *m/z* 219 peak. This is interpreted as being from an interaction of acetonitrile with the radical cation. Acetonitrile is a less powerful nucleophile than water, but is present in much higher concentration. If it were a nucleophilic addition, I would expect to see it at *m/z* 218. Instead, high energy collisions might be resulting in an electrostatic attraction between the cation and acetonitrile molecules. Beyond 160 V, all ion signals begin to drop, due to the neutralizing of charged molecules in high energy collisions.

From this study, it would appear that adducts, while initially present, are being both formed and destroyed in gas phase collisions before detection. In order to detect solution phase chemistry, the capillary voltage must be set low enough to limit gas phase collisions, while remaining high enough to efficiently transfer high mass adducts into the vacuum region of the mass spectrometer. Such a compromise may not be easy to obtain for higher mass adducts, and must be arrived at experimentally.

Hexapole Accumulation Time

The hexapole accumulates ions as they enter the vacuum region of the mass spectrometer and stores them until they are sent through the ion optics to the cell. The amount of time which ions are stored can influence the detected spectra as well. Longer storage times give increased sensitivity as ions accumulate. However, the longer molecules are stored in the hexapole, the more chance they have of colliding with other molecules and undergoing gas-phase reactions. In this experiment the ions were collected for periods from 0.1 up to 4 seconds. The signal strengths at each collection time are shown in Figure 4.10. Total ion signal strength increased with time up to 2 seconds and then stabilized. The radical cation remained the base peak up until 1 second, at which point the water adduct became the base peak. It appears that gas phase collisions do not
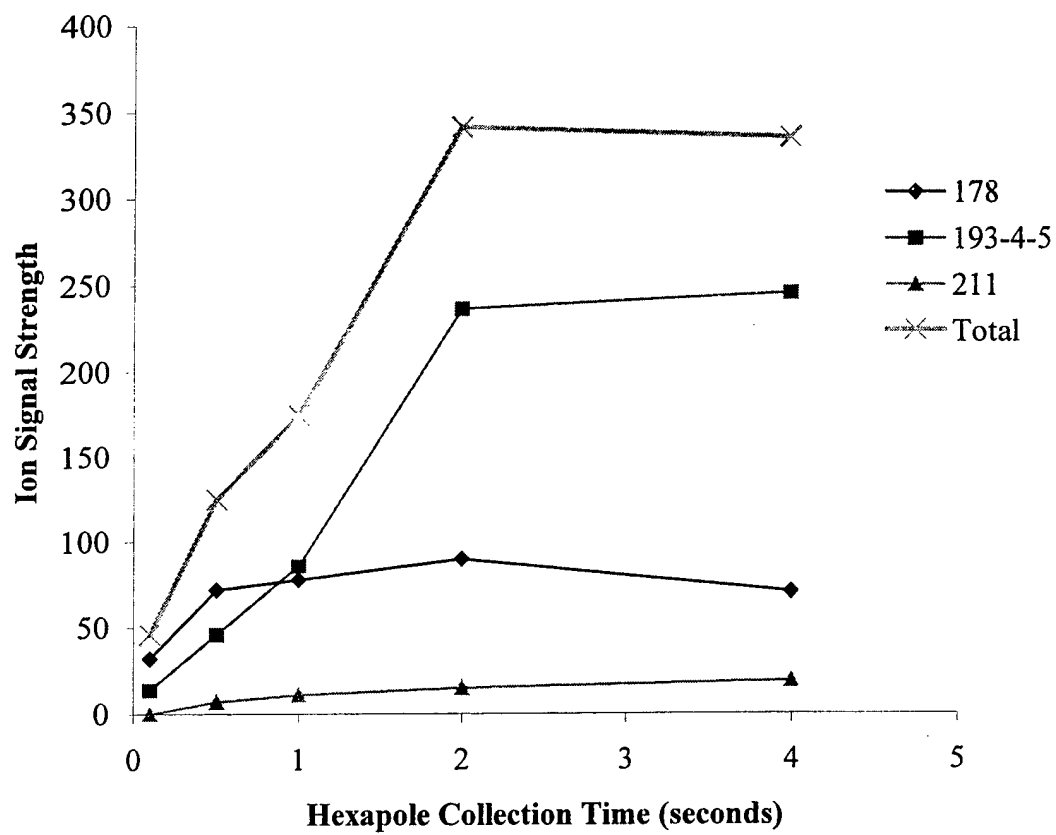
Figure 4.10. Ion signal strength with hexapole collection time.

significantly change the spectra until accumulation times of 2 seconds have been reached. This effect will vary with the total number of ions which is being trapped in the hexapole. To limit gas-phase reactions interfering with the detection of solution-formed adducts, accumulation times should be limited to 2 seconds or less in our system.

Reactions with Model Nucleophiles

I would like to use the electrospray process to study the reaction of PAHs with biological nucleophiles. Pyridine is a strong nucleophile and has been used as a model biological nucleophile for gas phase reactions with PAHs [Whitehill *et al.*, 1996]. The reaction of pyridine with anthracene in solution has been demonstrated in EC/ESI-MS to result in an anthracene-pyridine adduct with a *m/z* of 256 [Zhang, 2001]. In a series of experiments, the effect of the EC cell on this reaction was studied, along with the competition of this strong nucleophile with water in solution. Anthracene was again used as the PAH at a concentration of 1mM with 250 μM LiT in 50/50 acetonitrile/methylene chloride. Pyridine was added so that it made up 1% of the solution by volume. This ensured a higher pyridine concentration than the water or anthracene concentrations. The solution was sprayed in both the cell off and cell on mode at 5.0 V over a range of capillary voltages. A representative spectrum is shown in Figure 4.11 which shows the radical cation peak, the anthracene-water adduct peaks, and the anthracene-pyridine adduct at *m/z* 256. An additional peak at *m/z* 272 was observed, which is the adduct of anthracene with one water and one pyridine molecule.

The results of the experiment are shown in Figure 4.12. In both the cell off and the cell on mode, I observed that the pyridine adduct, *m/z* 256, is the base peak at low capillary voltage. When the capillary voltage increases to 100 V, there is a significant
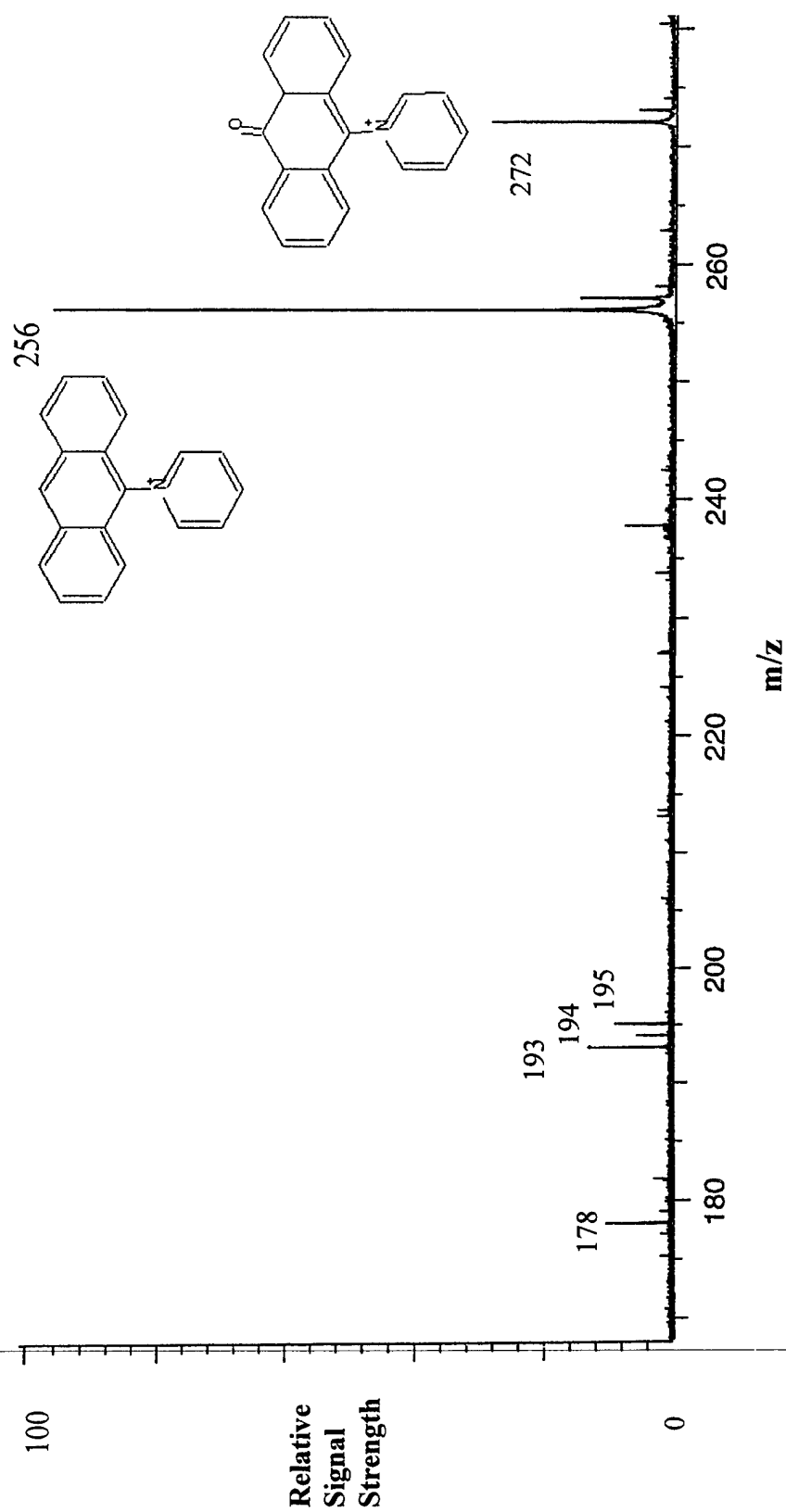
Figure 4.11. Anthrace -Pyridine adducts in EC/ESI-MS.
Conditions: 1mM anthracene, 250 μM LiT in 50/50 v/v ACN/MeCl$_2$, Pyridine 1% by volume
Flow rate: 75 μL/h, ESI voltage: 3.3 kV, Capillary voltage: 100 V, EC cell at 5.0 V.
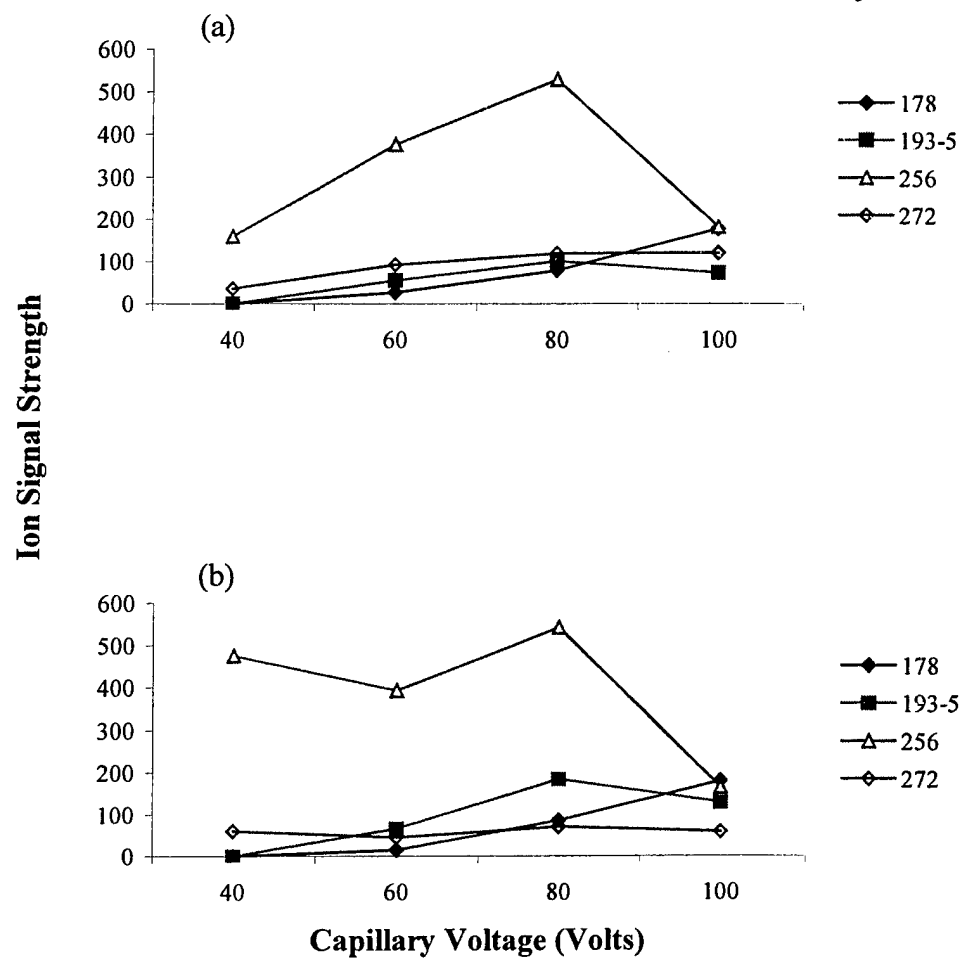
Figure 4.12. Anthracene-pyridine adducts with capillary voltage (a) ESI (b) EC/ESI.

decrease in 256 and a corresponding jump in 178. I postulate that the energy of gas phase collisions has increased and is sufficient to break the interaction between the pyridine and the anthracene, resulting in a decrease in the observed 256 signal and the corresponding increase in the radical cation. I find this to be the case in the cell on mode as well, although this mode produces a much more intense m/z 256 signal at low capillary voltages. In the cell off mode, cations are generated in the tip of the needle and have limited time to react in solution before they are sprayed. They react preferentially with the molecules which are the most nucleophilic and are in the highest concentration. The base peak will be due to this reaction, which is clearly with pyridine in both cases. However, some cations do not run into any nucleophiles before they are released into the gas phase. In the EC/ESI mode radical cations are generated well before (approximately 2 minutes in our system) they are sprayed. There is time for all cations generated at the EC cell to react with nucleophiles in solution before being electrosprayed. This results in much higher concentrations of adducted species observed in the EC/ESI spectra. High capillary/skimmer voltages promote the dissociation of adducts resulting in reduced signals at high capillary voltages for both cases. From this experiment, we can conclude that operating in the cell on mode has a distinct advantage for the observation of biological nucleophile adducts generated in solution. Again, the importance of operating at low capillary/skimmer differences was observed.

The detection of PAH adducts with DNA base nucleophiles necessitates generating charged adducts above the sensitivity limit of the instrument. These experiments demonstrate several considerations that must be made to increase the probability of adduct detection. First, concentrations of the intended nucleophile must be high enough

to make its reaction competitive with that of other nucleophiles in solution. Second, the EC cell can be employed to generate radical cations of the selected PAH before the ESI needle, extending the time for reaction in solution. Finally, ESI parameters must be carefully chosen to maximize the signal. Capillary voltages must be chosen for efficient transfer of the adduct being sought without causing significant dissociation.

DNA Base Adducts

Mass spectrometry has been used for the detection and identification of DNA base adducts which are generated off-line, including those formed in the electrolysis of PAH in the presence of a DNA base[Rogan et al., 1988]. The detection of DNA base adducts formed online may be useful to study the adduct forming potential of uncharacterized PAH or other suspect carcinogenic compounds. Since we have control over the oxidation of the PAH in the EC/ESI-MS instrument, we can learn the conditions under which a PAH might be activated. We can also learn the reactivity of the activated PAH with specific biological nucleophiles. The first step is to attempt to identify a PAH-DNA adduct formed online and enhance its detection. That step is explored in this section, by looking at solution composition effects and the use of the EC cell to generate a detectable PAH-DNA base adduct.

Solution Composition

Guanine was initially chosen as the DNA base for this study because the DNA adducts that have been detected are most often adducted to guanine bases [Rogan et al.,1988]. Guanine does not dissolve appreciably in either of the solvents which form the ESI solvent system. Strong acidic solutions are necessary for its solvation, making nonpolar solutions problematic. In the following experiments guanine was first dissolved in a 2 M solution of H_2SO_4. Small aliquots of this solution could be added to the 50/50

acetonitrile/methylene chloride solution. The acidic guanine solution is miscible to some extent in acetonitrile, but it is not miscible in methylene chloride. Only small amounts of guanine solution can be added before the components separate. These limitations contribute to a maximum guanine concentration of approximately 100 μM. This is a much lower concentration than that of either the water or the pyridine nucleophile in earlier studies, and is up to an order of magnitude lower than PAH concentrations. I would expect the DNA adduct signal to be very small under these conditions.

An additional consideration is that the sulfate and hydrogen ions act as electrolytes in solution. Since the concentration of H_2SO_4 must be higher than the concentration of guanine for sufficient solvation, adding small aliquots of guanine solution greatly increases the conductivity of the final solution. I observed that high concentrations of H_2SO_4 in solution caused the electrospray to become unstable, and no signal was observed. This also limits the amount of guanine that can be added to the PAH solution. As I worked with solutions to maximize the guanine concentration, I discovered that the acid electrolyte could be present in much higher concentrations than the LiT without causing suppression effects. In fact, it was found that LiT could be omitted entirely and only the H_2SO_4 used as electrolyte up to concentrations of 0.01 M. Figure 4.13 shows a 1 mM anthracene spectrum using only H_2SO_4 at 1 mM as electrolyte.

Anthracene-guanine adduct

In the anthracene and guanine study, guanine was observed in the mass spectrum as a protonated molecule at m/z 152. A mass peak could be detected at m/z 329 under cell on conditions, but not under cell off conditions. This prospective adduct had a higher mass number than I would expect based on the water and pyridine adducts in which
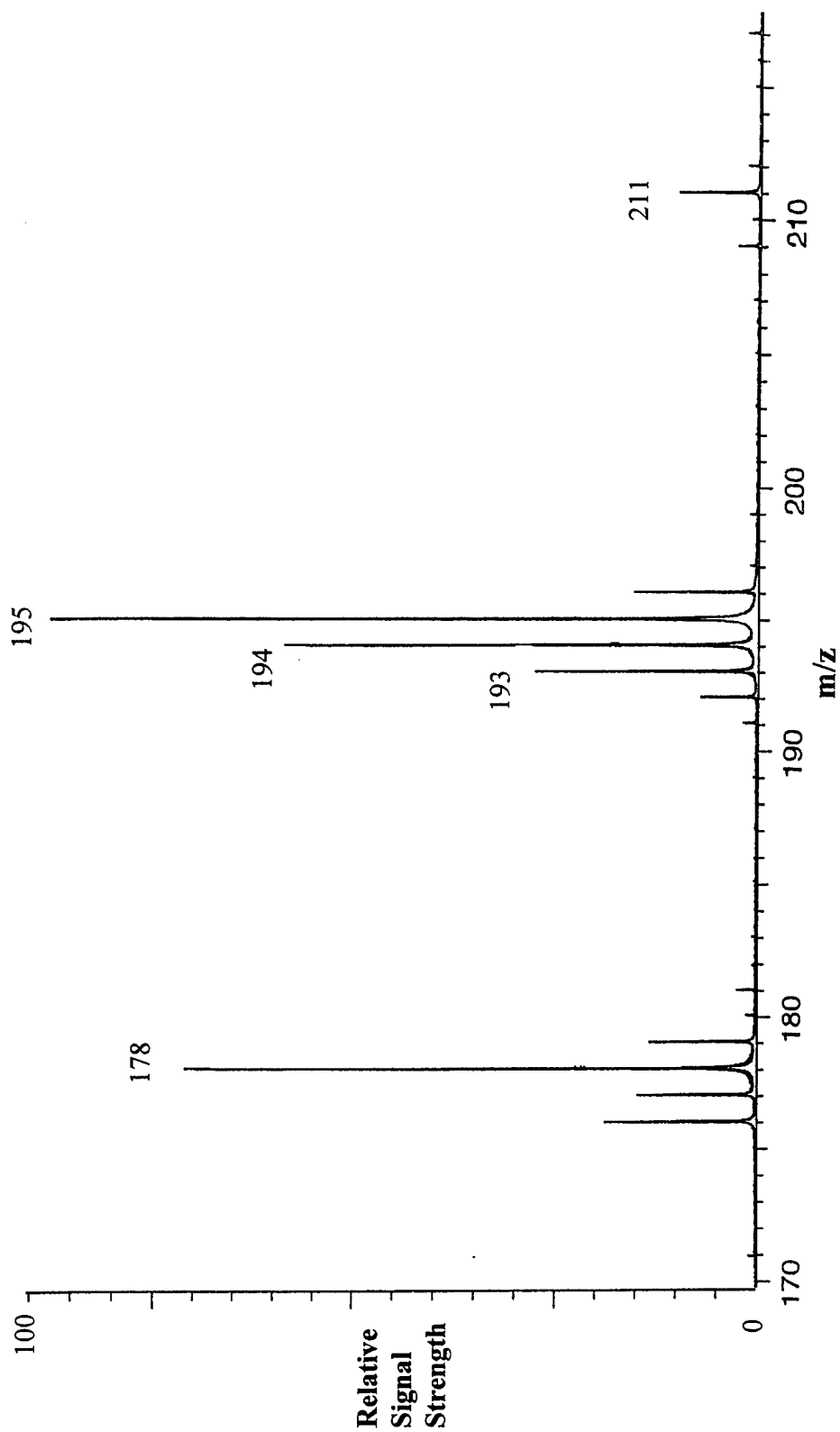
Figure 4.13. Anthracene spectrum using H_2SO_4 as electrolyte in ESI-MS. Conditions: 1mM anthracene, 1 mM H_2SO_4 in 49/49/2 v/v/v $ACN/MeCl_2/H_2O$ Flow rate: 75 µL/h, ESI voltage: 3.3 kV, Capillary voltage: 100 V.

anthracene loses a hydrogen when adducted. The peak at m/z 329 could be a result of the reaction of anthracene with protonated guanine, which accounts for the extra mass unit. The peak is very small compared to the surrounding peaks, many of which are chemical noise peaks and were unidentified. Spectra generated with solutions of guanine in H_2SO_4 contain many chemical noise peaks and it is difficult to assign peaks with certainty in the adduct region. A method of verifying the identity of the m/z 329 peak would be to enhance its detection, then isolate the peak and perform collision induced dissociation (CID) in the ICR cell to identify its components. Attempts to enhance the detection of this peak were unsuccessful, however. Several factors may contribute to the difficulty of this experiment. The first is the solubility of the DNA base in the solvent system. The concentrations of guanine may not be high enough to form detectable levels of reaction products. A second consideration is the reactivity of anthracene. Guanine nucleophiles may be unable to compete with the anthracene-water reaction since water is now present in much higher concentration in order to dissolve guanine. All anthracene cation radicals may be consumed in water reactions.

B[a]P-guanosine adduct

A second set of adduct experiments was performed using the PAH benzo[a]pyrene and the nucleoside guanosine as the nucleophile. Benzo[a]pyrene is a carcinogenic PAH and has been implicated in tumor initiation studies in rats [Searle ed., 1976]. The detection of ions in B[a]P's oxidative pathway shown in Figure 4.14 was performed by Xu *et al.* using EC/ESI-MS [Xu *et al.*, 1996]. A representative mass spectrum of 100 μM B[a]P with 250 μM LiT in 50/50 acetonitrile/methylene chloride is shown in Figure 4.15. Peaks were observed that correspond to the oxidation pathway of
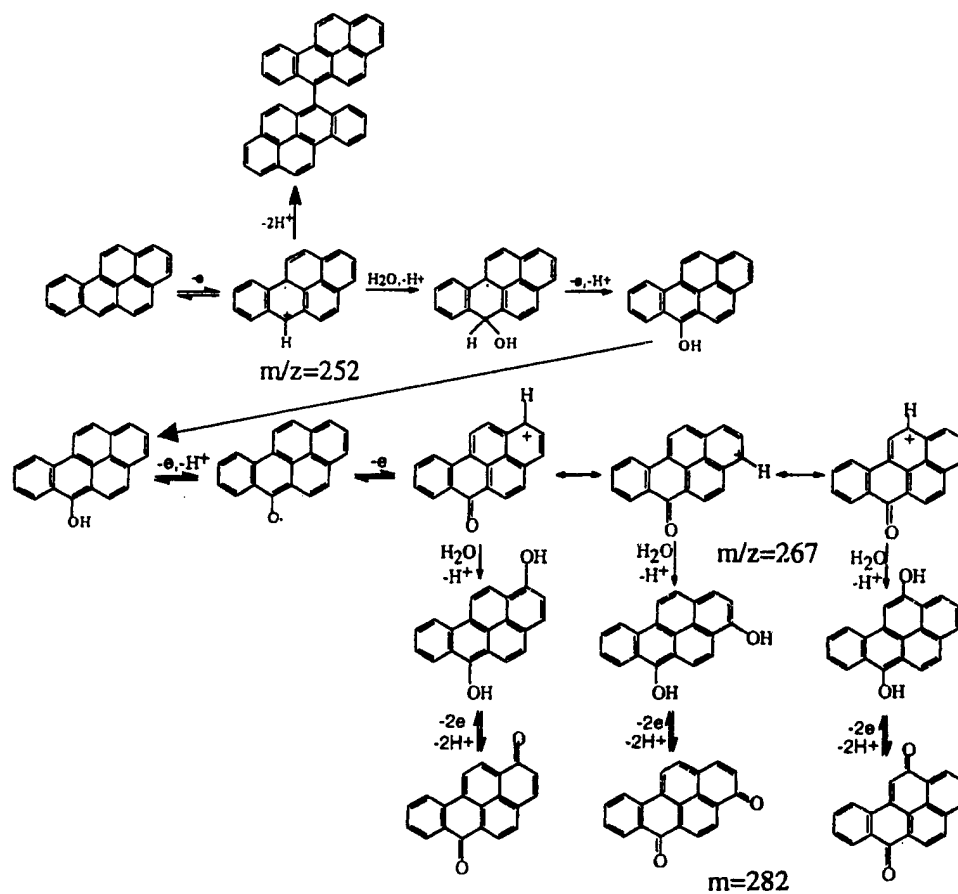
Figure 4.14. Benzo[a]Pyrene electrochemical oxidation pathway [Xu *et al.*, 1996].

B[a]P. The radical cation peak (m/z 252) and the mono- (m/z 267) and di-oxygenated (m/z 283) peaks are identified. B[a]P radical cations also react with the model biological nucleophile pyridine. When 1% pyridine is added to solution, the B[a]P-pyridine adduct is seen at m/z 330 as shown in Figure 4.16.

Guanosine is much more soluble in acid solution than guanine. A 0.01 M guanosine solution in 0.001 M H_2SO_4 was prepared. By changing the solvent mixture from 50/50 acetonitrile/methylene chloride to 80/10/10 acetonitrile/methylene chloride/water, I was able to add 1 mM guanosine to the solvent system without solvent separation. This resulted in guanosine concentrations that were an order of magnitude higher than those achieved in the guanine studies. The final H_2SO_4 concentration was only 100 μM, 100 times lower than in the guanine solutions, which contributed to more stable ESI conditions, and cleaner spectra. The mass spectrum of guanosine alone in solution is shown in Figure 4.17. The protonated guanosine peak, m/z 284, is the base peak. A protonated guanine peak at m/z 152 is also present. While this could be due in part to impurities in the guanosine sample, a study of these two peaks as a function of capillary voltage demonstrates that the glycosidic bond is being broken in gas phase collisions resulting in both guanine and guanosine in the mass spectrum. These peaks vary in signal strength as a function of capillary voltage.

To verify that DNA base adducts were being detected, I wanted to detect an adduct that has been previously reported. Adducts have been generated by the electrolysis of benzo[a]pyrene in solution with guanosine [Rogan *et al*, 1988]. These authors studied the products of the electrolysis of B[a]P with guanosine in solution and reported that the reaction of electrochemically oxidized B[a]P with guanosine predominantly yields an
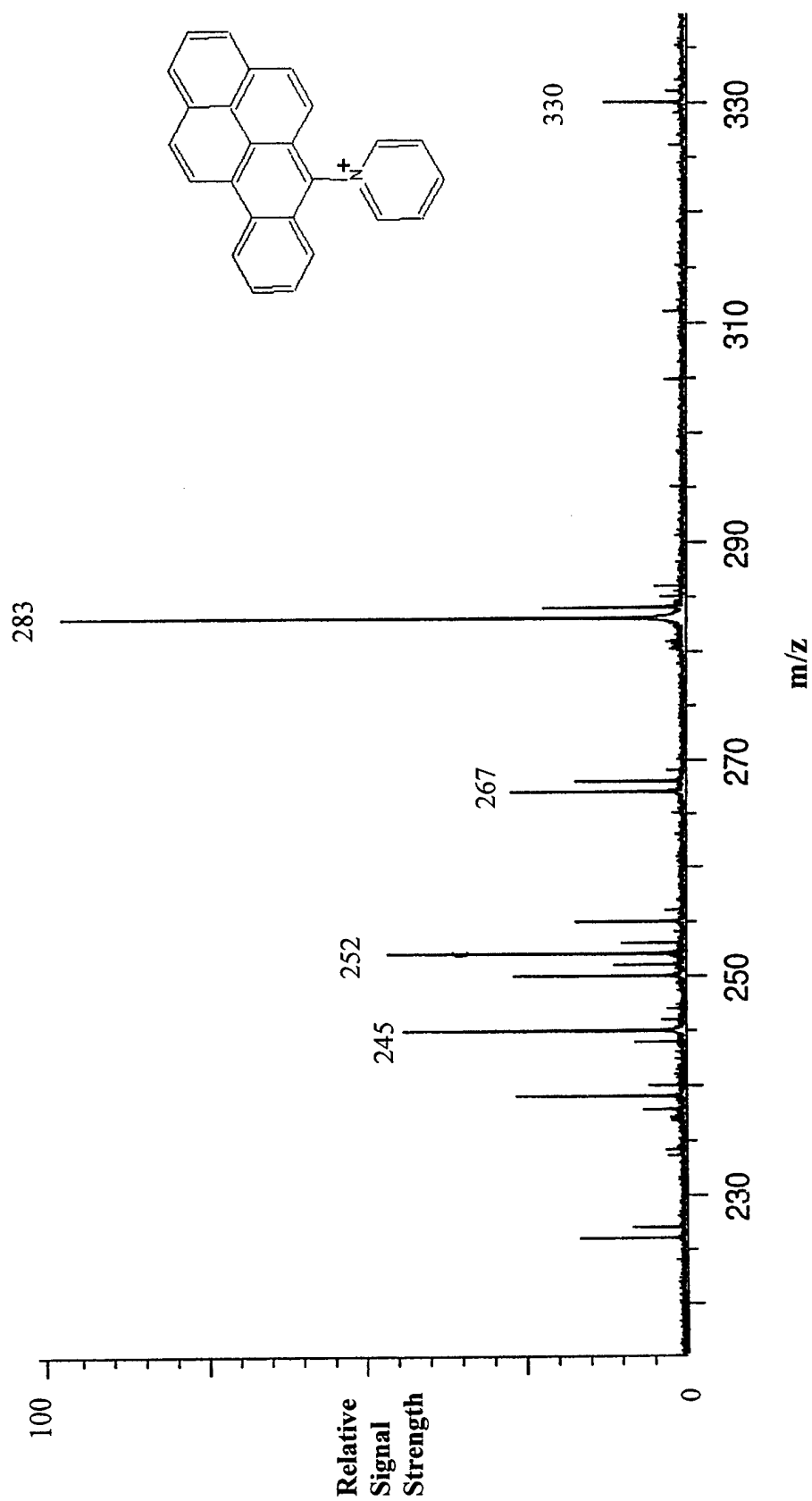
Figure 4.16. B[a]P and pyridine adduct in EC/ESI-MS.
Conditions: 100 μM B[a]P, 250 μM LiT in 50/50 v/v ACN/MeCl$_2$, added 1% pyridine by volume
Flow rate: 75 μL/h, ESI voltage: 3.3 kV, Capillary voltage: 100 V.
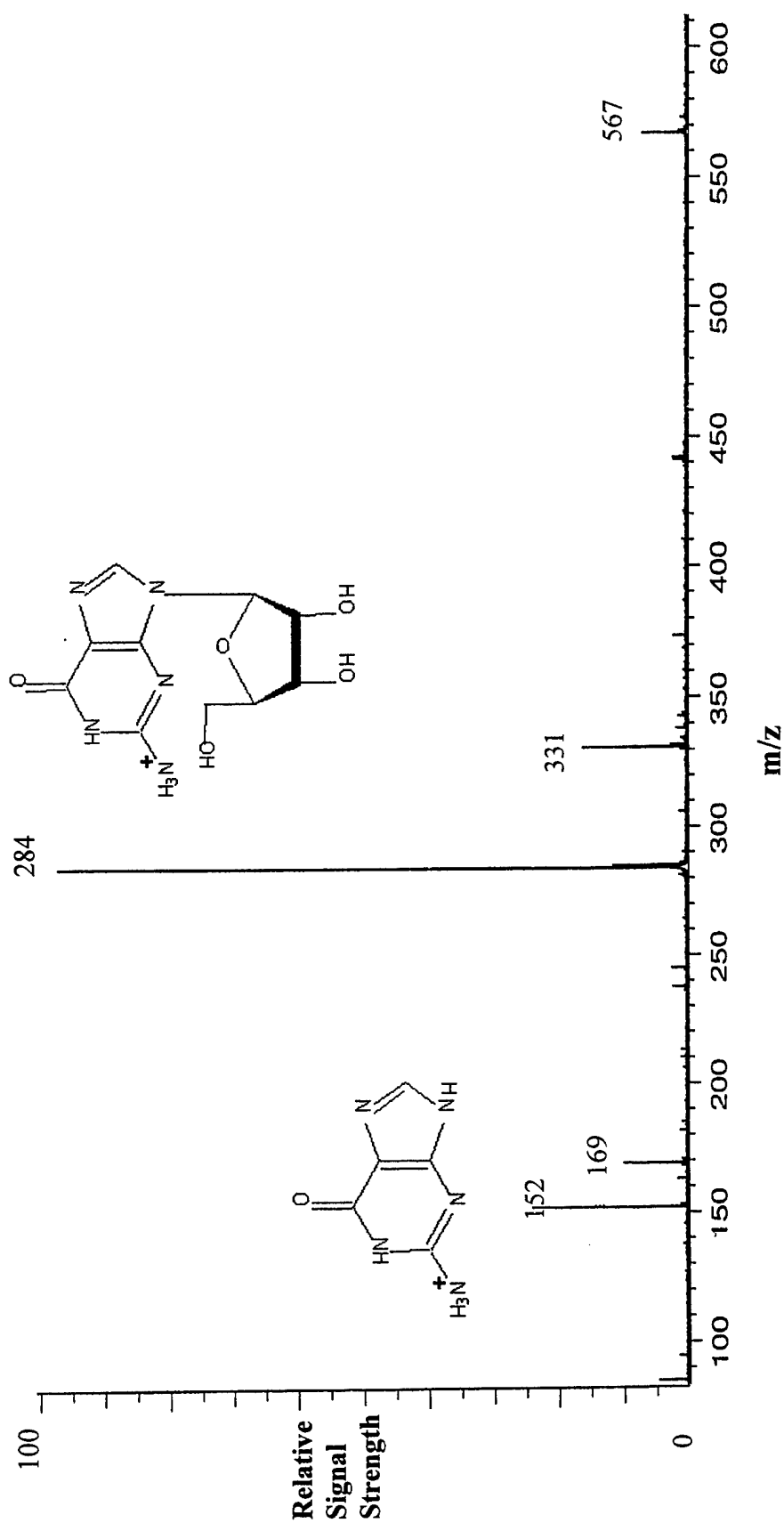
79

Figure 4.17. Guanosine spectrum in EC/ESI-MS.
Conditions: 1 mM Guanosine, 250 µM LiT, 100 µM H_2SO_4 in 80/10/10 v/v/v ACN/MeCl$_2$/H$_2$O
Flow rate: 60 µL/h, ESI voltage: 3.2 kV, Capillary voltage: 80 V.

adduct at the C8 carbon of guanosine [Rogan *et al.*, 1988]. This adduct was detected at *m/z* 534 using Fast Atom Bombardment (FAB) mass spectrometry. The species said to be detected was the [M+H]$^+$ ion. Both guanosine and B[a]P lose a hydrogen in the bond formation at C8. The molecule is detected when the amino group on the guanosine is protonated in FAB collisions. I detected a similar product, with the difference being that guanosine was already protonated in solution. The reaction at C8 results in the loss of two hydrogens and a final *m/z* of 534.

For this experiment, a solution of 100 μM B[a]P, 250 μM LiT, 1mM guanosine, and 100 μM H_2SO_4 in 80/10/10 acetonitrile/methylene chloride/water was sprayed at a flow rate of 60 μL/h. The high voltage was set at 3.2 kV and the capillary voltage was at 80 V. The spectrum obtained with the EC cell off is shown in Figure 4.18 along with the spectrum with the EC cell on mode at 5.0 V. A peak at *m/z* 534 appears in Figure 4.18b and is interpreted to be the B[a]P-guanosine adduct as previously detected by Rogan *et al.* [1988].

Conclusion

The results of this research support the conclusion that PAH-DNA bases can be generated in solution phase reactions and detected online in the EC/ESI-MS technique. However, the detected peak remains small and much more work could be done to optimize the signal achieved using this instrumental setup. Directions which might be immediately followed include increasing guanosine and B[a]P concentration in solution and removing as much water as possible from the solvent system to reduce this competing reaction.
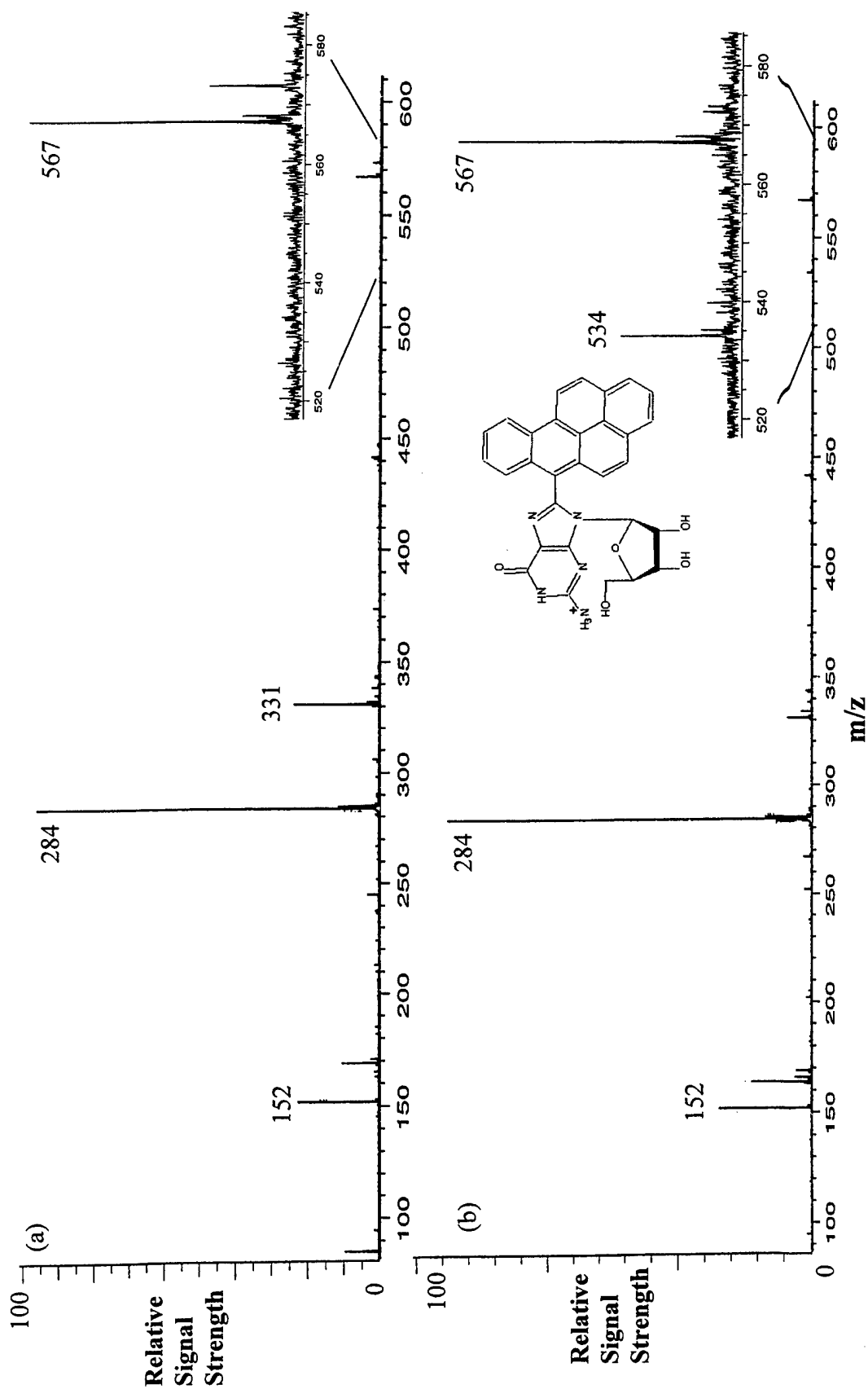
Figure 4.18. B[a]P and Guanosine spectrum (a) ESI-MS (b) EC/ESI-MS.
Conditions: 100 μM B[a]P, 1 mM Guanosine, 250 μM LiT, 100 μM H_2SO_4 in 80/10/10 v/v/v ACN/MeCl$_2$/H$_2$O
Flow rate: 60 μL/h, ESI voltage: 3.2 kV, Capillary voltage: 80 V.

Additional work on the composition of the solvent system might also improve results. If the solvent system could be made more polar to better reflect the environment of these reactions in the body, correlation between the ESI results and *in vivo* reactions might be more easily made. If the detection of adducts generated in solution phase proves to be reliable, the method may one day become a tool for evaluating the reactivity of oxidation activated compounds in the human body.

LIST OF REFERENCES

Alexandrov, M. L.; Gall, L. N.; Krasnov, M. V.; Nilolaev, V. I.; Shkurov, V. A.; *Zh. Anal. Khim.* **1985**, *40,* 1272.

Bard, A. J.; Faulkner, L. R. *Electrochemical Methods*; Wiley: New York, 1980.

Bartmess, J.E.; Phillips, L.R. *Anal Chem.* **1987**, *59,* 2012.

Blades, A. T.; Ikonomou, M. G.; Kebarle, P. *Anal. Chem.* **1991**, *63,* 2109.

Bond, A. M.; Colton, R.; D'Agostino, A.; Downard, A. J.; Traeger, J. C. *Anal. Chem.* **1995**, *67,* 1691.

Borgen, A.; Darvey, H.; Castagnoli, N.; Crocker, T. T.; Rasmussen, R. E.; Wang, I. Y. *J. Med. Chem.* **1973**, *16,* 502.

Brookes, P.; Lawley, P. D. *Nature,* **1964**, *202,* 781.

Bruckenstein, S.; Gadde, R. R. *J. Am. Chem. Soc.* **1971**, *93,* 793.

Bruins, A. P.; Covey, T. R.; Henion, J. D. *Anal. Chem.* **1987**, *59,* 2642.

Cavalieri, E.; Rogan, E. *Free Radicals in Biology*; Pryor, W., Ed.; Academic: New York, **1984**; *6,* 323.

Cavalieri, E.; Rogan, E.; Devanesan, P.; Cremonesi, P.; Cerny, R.; Gross, M.; Bopdell, W. *Biochemistry,* **1990**, *29,* 4820.

Cavalieri, E. L.; Rogan, E. G.; Roth, R. W.; Saugier, R. K.; Hakam, A. *Chem.-Biol. Interact.* **1983**, *47,* 87.

Chaudhary, A. K.; Nokubo, M.; Reddy, M.; Yeola, G. R.; Morrow, J. D.; Blair, I. A.; Marnett, L. J. *Science,* **1994**, *265,* 1580.

Cole, R. B. Ed.; *Electrospray Ionization Mass Spectrometry - Fundamentals, Instrumentation, and Applications*; John Wiley & Sons, Inc.: New York, 1997.

Conney, A. H. *Cancer Res.* **1982**, *42,* 4875.

Cook, J. W.; Hieger, I.; Kenneway, E. L.; Maynord, W. V. *J. Chem. Soc.* **1933**, 395.

Covey, T. R.; Bonner, R. F.; Shushan, B. I.; Henion, J. D. *Rapid Commun. Mass Spectrom.* **1988**, *2*, 249.

Cremonesi, P.; Rogan, E.; Cavalieri, E.; *Chem. Res. Toxicol.* **1992**, *5*, 346.

Deng, H.; Van Berkel, G. J. *Anal. Chem.* **1999**, *71*, 4284.

Devanaesan, P.; Rogan, E.; Cavalieri, E. *Chem.-Bio. Interact.* **1987**, *61*, 89.

Dole, M.; Mach, L. L.; Hines, R. L.; Mobley, R. C.; Ferguson, L.P.; Alice, M. B. *J. Chem. Phys.* **1968**, *49*, 2240.

Fearon, E. R. *Science* **1997**, *278*, 1043.

Ganem, B.; Li, Y. T. ; Henion, J. D. *J. Am. Chem. Soc.* **1991**, *113*, 7818.

Hambitzer, G.; Heitbaum, J. *Anal. Chem.* **1986**, *58*, 1067.

Hanson, A.; Rogan, E.; Cavalieri, E. *Chem. Res. Toxicol.* **1998**, *11*, 1201.

Hemminki, K.; Kskinen, M.; Rajaniemi, H.; Zhao, C. *Regul. Toxicol.Pharmacol.* **2000**, 32, 264.

Iannitti-Tito, P.; Weimann, A.; Wickham, G.; Sheil, M. M. *Analyst,* **2000**, *125*, 627.

Iribarne, J. V.; Thompson, B. A. *J. Chem. Phys.* **1976**, *64*, 2287.

Jurva, U.; Wikstrom, V. H.; Bruins, A. P. *Rapid Commun. Mass Spectrom.* **2000**, *14*, 529.

Kebarle, P.; Tang, L. *Anal. Chem.* **1993**, *65*, 972A.

Kriek, E.; Rojas, M.; Alexandrov, K.; Bartsch, H. *Mutation Research.* **1998**, 400, 215-231.

Loo, J. A.; Ogozalek, R. R.; Light, J. K.; Edmonds, C.G.; Smith, R. D. *Anal. Chem.* **1992**, *64*, 81.

Lu, W.; Xu, X.; Cole, R. *Anal. Chem.* **1997**, 69, 2478.

Lunn, R. M.; Zhang, Y. J.; Wang, L. Y.; Chen, C. J.; Lee, P. H.; Lee, C. S.; Tsai, W. Y.; Santella, R. M. *Cancer,* **1997**, *57*, 3471.

Majeski, E. J.; Stuart, J. D.; Ohnesorge, W. E. *J. Am. Chem. Soc.,* **1968**, 90, 633.

Marshall, A. G.; Hendrickson, C. L.; Jackson, G. S. *Mass Spectrom. Rev.* **1998**, *17*, 1.

Miller, E. C.; Miller, J. A. *Cancer*, **1981**, *47*, 2327.

Miller, J. A. *Cancer Res..* **1970**, *30*, 559.

Nestmann, E. R.; Bryant, D.W.; Carr, C.J. *Regul Toxicol. Pharmacol.* **1996**, *24*, 9.

Niessen, W. M. A. *Liquid Chromatography-Mass Spectrometry*, 2nd ed.; Marcel Dekker, Inc.: New York, 1999.

Olivares, J. A.; Nguyen, N. T. ; Yonker, C. R.; Smith, R. D. *Anal. Chem.* **1987**, *59*, 1232.

Palii, S. P.; Zhang, T.; Brajter-Toth, A.; Eyler, J. R. *Proceedings of the 49th ASMS Conference on Mass Spectrometry and Allied Topics;* 2001,

Peover, M. E.; White, B. S. *J. Electroanal.Chem.* **1967**, *13*, 93.

Pfeifer, R. J.; Hendricks, C. D. *AIAA J.* **1968**, *6*, 496.

Pretty, J. R.; Van Berkel, G. J *Rapid Commun. Mass Spectrom.* **1998**, *12*, 1644.

Pretty, J. R.; Deng H.; Goeringer D. E.; Van Berkel, G. J. *Anal. Chem.* **2000**, *72*, 2066.

Reddy, M. V. *Regul. Toxicol. Pharmacol.* **2000**, 32, 256.

Roberts, D. W.; Churchwell, M. I.; Beland, F. A.; Fang, J. L.; Doerge D. R. *Anal. Chem.* **2001**, *73*, 303.

Rogan, E.; Cavalieri, E.; Tibbels, S.; Cremonesi, P.; Warner, C.; Nagel, D.; Tomer, K.; Cerny, R.; Gross, M. *J. Am. Chem. Soc.* **1988**, *110*, 4023.

Rojas, M.; Alexandrov, K.; van Schooten, F.J.; Hillegrand, M.; Kriek, E.; Bartsch, H.; *Carcinogenesis*, **1994**, *15*, 557.

Sawyer, C. N.; McCarty, P. L.; Parkin, G. F. *Chemistry for Environmental Engineering* 4th ed.; McGraw-Hill, Inc.: New York, 1994.

Searle, C. S., Ed.; *Chemical Carcinogens, ACS Monograph 173* ; American Chemical Society: Washington D.C., 1976.

Solomons, T. W.; *Organic Chemistry, 5th ed.*; John Wiley & Sons: New York, 1992.

Smith, R. D.; Barinaga, C. J.; Udseth, H. R. *Anal. Chem.* **1988**, *60*, 463.

Tang, K. *Phys. Fluids* **1994**, *6*, 404

Taylor, G. I. *Proc. R Soc. London A* **1964**, *A280*, 383.

Thomson, B. A.; Iribarne, J. V. *J. Chem. Phys.* **1979**, *71*, 4451.

Van Berkel, G. J.; McLuckey, S. A.; Glish, G. L. *Anal. Chem.*, **1991**, *63*, 1098.

Van Berkel, G. J.; McLuckey, S. A.; Glish, G. L. *Anal. Chem.*, **1992**, *64*, 1586.

Volk, K. J.; Yost, R. A.; Brajter-Toth, A. *Anal. Chem.* **1992**, *64*, 21A.

Walker, V. E.; Fennell, T. R.; Upton, P. B.; Skopek, T. R.; Prevost, V.; Shuker, D. E.; Swenber, J. A. *Cancer Res.* **1992**, *52*, 4328.

Walton, M.; Egner, P.; Scholl, P. F.; Walker, J.; Kensler, T. W.; Groopman, J. D. *Chem. Res. Toxicol.* **2001**, *14*, 919.

Watson, J. T. *Introduction to Mass Spectrometry 3rd ed.;* Lippincott-Raven: Philidelphia, 1997.

Whitehill, A. B.; George, M.; Gross, M. L. *J. Am. Soc. Mass Spectrom.* **1996**, *7*, 628.

Whitehouse, C. M.; Dreyer, R. N.; Yamashita, M.; Fenn, J. B. *Anal. Chem.* **1985**, *57*, 675.

Xu, X.; Lu, W.; Cole, R. *Anal. Chem.* **1996**, *68*, 4244.

Yamashita, M.; Fenn, J. B. *J. Phys. Chem.* **1984**, *88*, 4451.

Yamashita, M.; Fenn, J. B. *J. Phys. Chem.* **1984**, *88*, 4671.

Zeleny, J. *Phys. Rev.* **1917**, *10*, 1.

Zhang, T. *Dissertation.* University of Florida, **2001**.

Zhang, T.; Brajter-Toth *Anal. Chem.* **2000**, *72*, 2533.

Zhang, T.; Palii, S. P.; Eyler, J. R.; Brajter-Toth, A. *Anal. Chem.* **2002**, in press.

Zhou, F.; Van Berkel, G. J. *Anal. Chem.* **1995**, *67*, 3643.

BIOGRAPHICAL SKETCH

David Pfahler was born in the town of Bucyrus, Ohio, on December 27, 1973. He received a Bachelor of Arts degree in chemistry from Cedarville College in Ohio and an Officer's Commission in the United States Air Force in June of 1997. On September 27, 1997, David married the love of his life, Alicia Marie Elmore. They moved to New Mexico where David worked for three years at the Gas and Chemical Laser Branch of the Air Force Research Lab. In March of 2000 he was selected to pursue a master's degree in chemistry and chose to attend the University of Florida studying analytical chemistry. While in Florida, David and Alicia were blessed with a beautiful gift, Annalese Joy, who was born on December 18, 2000. David completed his research and received a Master of Science degree in May 2002.